Graduate School ETD Form 9
(Revised 12/07)

PURDUE UNIVERSITY
GRADUATE SCHOOL
Thesis/Dissertation Acceptance

This is to certify that the thesis/dissertation prepared

By Kellen A. Knowles

Entitled

Adipose Stromal Cells Enhance Keratinocyte Survival and Migration In Vitro, and Graft Revascularization In Mouse Wound Healing Model

For the degree of Master of Science in Biomedical Engineering

Is approved by the final examining committee:

Keith March
Co-Chair

Edward Berbari
Co-Chair

Julie Ji

To the best of my knowledge and as understood by the student in the *Research Integrity and Copyright Disclaimer (Graduate School Form 20)*, this thesis/dissertation adheres to the provisions of Purdue University's "Policy on Integrity in Research" and the use of copyrighted material.

Approved by Major Professor(s): Keith March

Approved by: Edward Berbari 06/17/2013
Head of the Graduate Program Date

ADIPOSE STROMAL CELLS ENHANCE KERATINOCYTE SURVIVAL AND MIGRATION *IN VITRO*, AND GRAFT REVASCULARIZATION IN MOUSE WOUND HEALING MODEL

A Thesis

Submitted to the Faculty

of

Purdue University

by

Kellen Alexander Knowles

In Partial Fulfillment of the

Requirements for the Degree

of

Master of Science in Biomedical Engineering

August 2013

Purdue University

Indianapolis, Indiana

I dedicate this thesis to my father, Daniel Alexander Knowles and my mother, Sherle Arlene Major-Knowles. They taught me the value of hard work and dedication. Love you both!

ACKNOWLEDGMENTS

I have been the product of many valuable investments, for which I am grateful. Thus this list is a long one, but is by no means exhaustive. First, I'd like to thank Dr. March, the co-chair of my committee and my mentor. Your wisdom, patience and standards of excellence have helped motivate me to reach this point. Dr. Dmitry Traktuev, you have served a pivotal role in my progress during my years in the lab. Your love for the science, availability, commitment, and motivation have been a significant help to me. Many thanks to Steffi Merfeld-Clauss for always being willing to support my work by providing cells, inspecting the quality of my cell work or teaching me new protocols. Special thanks to Michele Schlegelmilch for her administrative support, but most importantly, for being a friend and a good sanity check. I will miss you! Thanks to Todd Cook for his support with our animal study. To all others in the March, Murphy and Clauss labs; all of you have helped contribute to me reaching this point. Thanks for your encouragement, help and wisdom. Thanks to Dr. Rajiv Sood for initiating and supporting this project by providing access to the wound healing material. To the other co-chair of my committee, Dr. Berbari, thanks for your tough love, patient motivation and for believing in me. Dr. Ji, I know I made a great choice when I asked you to be on my committee. Thanks for being so understanding and for helping me to think through the small, but important things. Many thanks to Michael Wilson, my biostatistical consultant for generating statistical power data and building the ANCOVA model for the data analysis. Dr. Sunil Tholpady, your knowledge of the field of wound healing, friendliness, approachability and availability were greatly appreciated. Many thanks also for providing us access to wound healing material. To Valerie Lim-Diemer, thanks for providing your thesis formatting support and providing valuable input and advice along the way. To Shelly Albertson, thanks for always being a friendly face in the BME Department. All the things you do for

us students are invaluable. To the IU Pathology and Histology labs, many thanks for your work in preparing and staining my tissue samples.

To some of the previous mentors, advisors and professors that have had an impact on my life at IUPUI such as Dr. Karen Alfrey, Dr. Jack Windsor, Dr. Terri Talbert-Hatch, Marilyn Mangin, Cynthia Murdock, Lisa Ruch, Melissa Biddinger, Dr. Lin Zhu, and many others: Words are not enough to express my gratitude. The impact you have had on my life and on helping me get to this place has been monumental. Thank you! My maternal grandparents, Emerson and Betty Major, you all have been some of my biggest fans. Thanks for believing in me, and for all your love and support over the years. To my paternal grandparents James and Ethelyn Knowles (deceased), I love and miss you all! To my uncle Kendall, thanks for always taking an interest in my life and career path. I love you and am proud of you! My myriad of friends, you all are the best! Thanks for all of you that contributed to this laptop that I'm now using to write my thesis. I still can't get over the huge surprise it was! I'm truly a blessed man. Jesse and Jeremy, you guys are some of the best brothers a guy could wish for. You've taught me so much and been there for me when it really mattered. Love you both! To my friend, Laurie Filson, thanks for supporting me even in your absence. Your faithful prayers and encouragement through these times have meant alot. Can't wait to see you again! Ronaldo, and Trevor, I love you my friends. Look forward to many more good times! Daryl and Khadijah, my wonderful sisters, thanks for teaching me to be a better brother and a better man.

To my parents, Daniel and Sherle Knowles, I dedicate my thesis to you. You all are some of the best parents a son could wish for! Thanks for all the sacrifices, you made to help make Jarrod and I become more successful in our careers and in our faith. I love you both and hope we can continue to make you all proud. Jarrod, my brother, thanks for believing in me. I'm proud of all of your accomplishments! Finally, and most significantly, to my Abba, we know none of this is possible apart from You. Thanks for calling me out of a dark, meaningless life into a life of purpose, light and abundant life in Your Son, Jesus Christ. I live for Your smile.

TABLE OF CONTENTS

Page

Page

LIST OF FIGURES

Figure Page

Figure Page

ABSTRACT

Knowles, Kellen Alexander. M.S.B.M.E., Purdue University, August 2013. Adipose Stromal Cells Enhance Keratinocyte Survival and Migration *in vitro*, and Graft Revascularization In Mouse Wound Healing Model. Major Professor: Keith L. March.

In the US, more than 1 million burn injuries are reported annually. About 45,000 injuries due to fires and burns result in hospitalization and ten percent of these result in death every year. Advances in burn treatment have led to a reduction in mortality rate over the last decades. Since more patients are surviving the initial resuscitation phase even with very large areas of skin being burned away, wound care has become increasingly important to ensure continued patient survival and improvement.

While currently a common treatment for third degree burn wounds, skin grafts have several drawbacks. The availability of donor sites for autografts may be limited, especially in incidences of extensive skin loss. The rejection associated with the use of allografts and xenografts may render them inadequate or undesirable. Even if a suitable graft is found, poor retention due to infection, hematoma, and low vascularity at the recipient site are other drawbacks associated with the use of skin grafts as a primary treatment for severe burn wounds. As such, research has been done into alternative treatments, which include but are not limited to artificial skin, cell therapy, and growth factor application.

We propose the delivery of adipose derived stem cells (ASC) in combination with endothelial progenitor cells (EC) via Integra Dermal Regenerative Template (DRT) to promote faster graft vascularization and thus faster healing of wounds. Integra DRT is an acellular skin substitute that consists of a dermal layer composed of bovine collagen and chondroitin-6-sulfate glycosaminoglycan, and an "epidermal" layer, which consists of silicone polymer. This silicone layer is removed after the collagen matrix

is adequately vascularized (usually takes 2-3 weeks), and then a thin layer autograft is applied to the top of the neo-dermis. ASC are derived from the stromal-vascular fraction (SVF) of adipose tissue and are a readily available, pluripotent, mesenchymal cell known to promote angiogenesis. They are being explored as a treatment for a myriad of diseases and conditions, including wound healing. In combination with ECs, they form stable microvessel networks in vitro and in vivo.

In our work, we found that ASC+EC form stable microvessel networks when cultured on Integra DRT. Also, ASC and ASC+EC conditioned media promoted both survival and migration of human epidermal keratinocytes compared to control medium. In a full thickness wound healing model, using healthy NSG mice, the ASC+EC case showed a significantly higher rate of wound closure compared to control. Based on best linear unbiased estimates (BLUE), the difference between the healing rates of ASC alone treatment and the Control treatment group is -0.45 +/- 0.22 mm^2/day (p=0.041), which is not less than 0.025 and thus not statistically significant (Bonferroni Adjusted). However, the BLUE for the difference between the ASC+EC group and the Control group healing rates is -0.55 +/- 0.28 mm^2/day (p = 0.017 $<$ 0.025, Bonferroni Adjusted), which is statistically significant. Histology revealed a significantly higher number of vessels compared to control in both ASC alone and ASC+EC case. CD31 staining revealed the presence of human vessels in ASC+EC treatment scaffolds.

We conclude that the combination of ASC and EC can be used to accelerate healing of full-thickness wounds when delivered to site of the wound via Integra. This result is especially compelling due to the fact that the mice used were all healthy. Thus our treatment shows an improvement in healing rate even compared to normal wound healing.

1. INTRODUCTION

Wound healing therapy dates back as far as 2000 B.C. with the Sumerians who applied a poultice-like material to wounds to aid in healing [1]. Around 1500 BC the ancient Egyptians and Grecians used honey, lint and animal grease as topical treatments for wounds [1, 2]. The honey served as an antimicrobial agent. The lint was an absorbent, and the grease served as a barrier to pathogens [1, 2]. Today, with such novel advancements as bioengineered skin substitutes, negative pressure therapy, hyperbaric oxygen therapy, and stem cell based therapies (to name a few), we have come a long way [3, 4]. However, many of the basic principles of wound healing treatments remain the same.

In this paper we focus on the combination of adult stem cells with bioengineered skin substitutes to aid in treatment of third degree burn wounds.

1.1 Structure of Skin

The skin is constantly exposed to stresses from the surrounding environment (mechanical, thermal, microbiological, chemical, etc.) [5]. Mammalian skin functions to protect underlying tissues on many levels and has thermo- and osmo-regulatory functions [6]. With such important roles, the skin's ability to regenerate and heal is crucial.

Skin consists of an outer epithelium and inner connective tissue layer [5, 7]. The epithelium, known as the epidermis is avascular. It consists of several layers of keratinocytes, which form a waterproof barrier to protect the underlying tissue and prevent water loss [5, 7]. Epidermis regenerates readily when injured, provided the underlying dermis is not affected [5, 7]. The connective tissue layer consists of the dermis and hypodermis. The collagen-rich dermis is vascularized and contains elastic

fibers, hair follicles, oil glands, sweat glands, fibroblasts and nerve endings, all of which help skin fulfill its protective and regulatory roles [7]. The dermis provides the structural support and strength of the skin [7]. If a wound results in bleeding, this indicates damage to the dermis [7]. The hypodermis is a fatty layer that provides support and padding to the skin [5, 7].

1.2 Healing Process

The process of wound healing involves 4 major steps including hemostasis, inflammation, proliferation, and remodeling. These phases are interactive and overlap in the healing process [8,9]. Hemostasis is marked by vasoconstriction and fibrin clot formation [8,9]. Platelets adhere to the injured epithelium to help plug the breach in the vessel wall [8,9]. The clot, along with surrounding wound tissue, secrete chemokines that help initiate the inflammatory response [8–10]. The inflammatory phase is marked by vasodilation and an increase in vascular permeability. Neutrophils, macrophages, and lymphocytes are attracted to the wound site [8, 9]. Neutrophils target invading microbes and cellular debris [8]. Macrophages are a phagocytic cell that clear away cellular debris, produce various chemokines and growth factors, and play a key role in initiating the proliferative phase [8, 9, 11]. T-lymphocytes, assist in regulating the inflammatory phase, and target pathogens via cell-mediated immunity [8].

The proliferative phase is marked by re-epithelialization, angiogenesis, ECM formation, and synthesis of collagen [8]. The remodeling phase, which can last for years, is characterized by a restoration of normal vascular density, wound contraction, and ECM remodeling. At each step in the healing process cytokines, chemokines, and growth factors help direct wound healing events. The goal is the restoration of cellular structures and tissue layers.

1.3 Burn Wounds

In the US, more than 1 million burn injuries are reported annually [12–14]. About 45,000 injuries due to fires and burns result in hospitalization and ten percent of these result in death every year [14].

Advances in burn treatment have led to a reduction in mortality rate over the last decades [14,15]. Since more patients are surviving the initial resuscitation phase even with very large areas of skin being burned away, wound care has become increasingly important to ensure continued patient survival and improvement [14,15].

Burn wounds are classified according to the depth of the injury. Superficial wounds that affect just the epidermis are known as first degree burn wounds and require no surgical intervention [16]. Second degree burn wounds include damage to the epidermis and dermis and may need to be debrided, treated with antibiotics and dressed with a wound dressing [16]. Third degree burn wounds are ones in which both the epidermis and dermis are damaged or destroyed. In most cases they must be treated via surgical debridement and skin grafting [16]. With the dermis and epidermis damaged, the skin has limited ability to regenerate itself and will result in extensive scarring if left treated [17].

1.3.1 Current Clinical Treatments

Skin grafting is a surgical procedure that involves taking skin from one area of the body and using it to cover and stimulate healing in the injured portions of skin [18]. Presently, the only effective treatment for severe second degree and third degree burn wounds is a skin graft or use of artificial skin [16, 18]. In adults, the dermis has limited ability to regenerate unaided, so deep wounds, if left untreated, will heal by scar tissue formation or in some cases, not at all [17]. Open wounds are highly susceptible to infection [16, 19]. The longer the wound is open the longer the risk remains. If infection does develop, this will lead to an even slower healing and can cause other complications, including death [16].

If the graft is taken from the patients own skin it is known as an autograft. If the available skin on the patient is unsuitable for use as a graft, or if there is an insufficient amount of skin available for forming the graft, skin can also be used from another person (allograft) or organism (xenograft). These will only serve as temporary solutions since the body will eventually reject them. There are several types of skin grafts [18]:

1. Pinch grafts: quarter inch pieces of skin that are spaced around site of injury. They eventually grow and spread, making larger and larger islands of new skin.

2. Split-thickness grafts: sheets of mostly superficial and some deep layers of skin that are used to cover non weight bearing portions of the body.

3. Full-thickness grafts: same as above except composed of deep layers of skin. Used for weight-bearing and friction prone areas such as feet and joints.

The recipient site is prepared for the skin graft by debridement or removal of dead and necrotic tissue. Favorable surfaces for skin graft take include briskly bleeding dermis or glistening fat [18]. If necessary, debridement can be done down to the muscle layers [18].

1.3.2 Drawbacks and Limitations of Skin Graft Treatments

While currently a common treatment for third degree burn wounds, skin grafts have several drawbacks. The availability of donor sites for autografts may be limited, especially in incidences of extensive skin loss [14, 16, 20]. If this is the case, repeated harvesting is necessary, and this is associated with pain and scarring at the donor site [14]. The rejection and possible transfer of infection associated with the use of allografts and xenografts may render them inadequate [20]. Poor graft retention due to infection, hematoma, and low vascularity at recipient site are other drawbacks associated with the use of skin grafts as a primary treatment for severe burn wounds [21]. As such, research has been done into the use of artificial skin substitutes as a

burn treatment. They are readily available, non-immunogenic, encourage in-growth of surrounding cells, and can be loaded with specialized cells or growth factors that stimulate faster healing, prevent fluid loss, and reduce scarring [17, 20, 21].

1.3.3 Skin Substitutes

Skin substitutes serve as a readily available treatment for burn wounds. They can be subdivided into three major categories: acellular, cellular and cellular autologous [20].

Three examples of acellular skin substitutes include Biobrane, Integra and Alloderm [14, 20]. Biobrane is a temporary skin substitute, which consists of a nylon mesh and semi-permeable silicone backing. Collagen is chemically linked to the nylon and silicone matrix, which improves its adherence to the wound bed. The Biobrane matrix is removed once the wound is healed or when autograft skin becomes available [14, 20]. Integra Dermal Regeneration Template consists of a dermal layer composed of bovine collagen and chondroitin-6-sulfate glycosaminoglycan, and an "epidermal" layer, which consists of silicone polymer [14]. The collagen matrix encourages ingrowth of cells from the wound bed [14]. This repopulation leads to eventual collagen matrix remodeling [14]. The silicone layer is removed after the collagen matrix is adequately vascularized, and then a thin layer autograft is applied to the top of the neo-dermis [14, 20]. Alloderm is composed of decellularized human dermis derived from cadavers [14]. It is treated so that it maintains native dermal structure, which facilitates cellular ingrowth and remodeling [14, 20].

Examples of cellular-based skin substitutes indicated for use in burn treatment include Transcyte [14,22] and OrCel [14,20]. Transcyte is a temporary wound covering for burns and is composed of nylon and a silastic membrane [14,20]. Neonatal foreskin-derived fibroblasts are seeded onto the nylon mesh and allowed 3-6 weeks to produce extracellular matrix and growth factors. However, in order to prevent an immune response, the fibroblasts are destroyed before Transcyte is applied to the wound.

Orcel is a skin graft composed of a type I collagen sponge that contains epidermal keratinocytes and dermal fibroblasts [14, 23]. It is indicated for use in treating donor sites from which skin grafts are obtained [14, 23]. The allogeneic cells serve a purpose in secreting factors and stimulating the healing process, but are eventually destroyed by the host [23].

The skin substitutes discussed above have the advantage of being readily available. However, they will eventually require replacement by the patient's own cells [14]. Their benefit is that they can be used to help facilitate wound closure while autologous cells are prepared for grafting [14].

Epicel, also known as cultured epidermal autograft (CEA) is an example of a cellular autologous skin substitute. It consists of sheets of autologous keratinocytes that were originally obtained from a skin biopsy taken from the patient, that has been expanded in culture [14]. The cells are seeded onto a petrolatum gauze backing that is removed about 1 week after graft is applied to the wound [14]. Epicel has been useful in treating patients with a total burn surface area (TBSA) of 60% or greater [14, 24]. Epicel has the advantage of being autologous, compared to other treatments, however, disadvantages include mechanical fragility, and obvious time needed for cell expansion (16-21 days) [14, 24, 25].

One of the most important factors in successful wound closure is timely and efficient vascularization of the skin graft. Poor graft revascularization is one of the highest contributing factors to graft failure [26]. Combining an acellular skin graft with a readily available, autologous cell or combination of cells that promote rapid and robust vascularization is one possible approach to addressing this issue. Adipose Stromal Cells (ASCs) are one such cell that have been shown to stabilize formation of vascular networks formed by endothelial cells [27].

1.4 Description of Adipose Stromal Cell Biology

Adipose Stromal Cells (ASC) are a population of pluripotent, mesenchymal stem cells, derived from the stromal-vascular fraction of adipose tissue. Traktuev, et.al, showed that the majority of CD34+ cells in the fat tissue were associated with vessels in the tissue [28]. While some CD34+ cells co-expressed CD31 (marker for endothelial cells), the predominant population is CD31-. The perivascular position of this latter population, suggests their pericytic function [28]. Upon isolation, it was found that the majority of CD34+/CD31-/CD45-/CD144- cells defined as ASC, also express mesenchymal cell markers, such as CD10, CD13, and CD90, as well as pericyte markers - CD140a, and CD140b (PDGF receptor-α and -β, respectively) [28].

It has been shown that ASC possess high plasticity and are able to differentiate into adipocytes, osteocytes, chondrocytes, hepatocytes, neurons and cardiomyocytes [29]. ASC are easily obtained through lipoaspiration or abdominoplasty, both minimally invasive procedures compared to MSC harvesting from bone marrow [28]. In a study conducted by Harris, et.al, it was shown that advanced age (greater than 70 years), gender, BMI, diabetes mellitus, and peripheral vascular disease did not significantly affect ASC density in the fat tissue [30]. For many of these reasons, ASC are gaining more attention in the areas of tissue engineering and cell therapy.

1.4.1 ASC Support Formation of Robust Vascular Networks When Co-seeded With EC

Traktuev, et.al. found that while cord blood-derived Endothelial Cells (EC) were sufficient to form functional vessels in mice, the vessels were limited in number and persistence [27]. When the EC were co-seeded together with ASC in vitro and in in vivo collagen implants, ASC were found to function in a pericytic manner by surrounding and stabilizing functional microvessel networks formed by EC. ASC not only increased stability but also the number of functional vessels formed by EC [27].

The ASC exerted their effect via direct contact and by secretion of various angiogenic and anti-apoptotic factors [31, 32].

1.5 ASC Promote Keratinocyte Survival and Wound Closure

ASC have been shown to possess therapeutic potential in the healing of cutaneous wounds. In previous studies done in our lab, Blanton et. al. found that while ASC+plasma (either platelet rich or platelet poor) delivered in a fibrin gel to full-thickness wounds in pigs did not show an increase in wound closure rate, compared to saline control, both types of plasma vehicles containing ASC, stimulated an increase in vascular density in their respective wound beds [33]. However the combination of platelet-rich plasma (PRP) with ASC showed the greatest improvement in wound cosmesis. Increased VEGF accumulation in the wound bed was observed in all treatments containing ASC. The lack of observed effect on re-epithelialization was attributed to the fact that improving healing in normal, healthy, skin is often difficult to observe. This study was further extended by Hadad et. al., who found that ASC + platelet-rich plasma delivered in a fibrin gel to full-thickness wounds in an irradiated (delayed wound healing) porcine model, showed an increase in microvessel density and in wound closure rate compared to saline control [34].

The incidence of cutaneous wounds, such as foot ulcers, is on the rise due to an increased incidence of diabetes. Amos, et.al showed that ASC applied to full-thickness wounds in a diabetic mouse model (leptin receptor deficient db/db mice) significantly improved healing compared to diabetic control. ASC were delivered as multicellular aggregates [35].

Nie, et.al, showed that ASC administered locally via intradermal injections to a full-thickness cutaneous wound resulted in faster wound closure in both normal and diabetic mice. It was found that in the wound site there was an increase in the pro-angiogenic cytokines HGF and VEGF in ASC treated wounds. They also saw evidence of ASC incorporation into regenerated epidermal structures and differentiation into

vascular structures [36]. Nie, et.al. also showed that ASC delivered to the site of excisional wounds in diabetic rats using Acellular Dermal Matrix (ADM), increased wound closure rate via increased epithelialization and tissue regeneration. There was also increased capillary density and increased expression of angiogenic factors in wounds receiving ASC-ADM grafts compared to controls [37].

Kim et.al. showed that the application of ASC to cutaneous wounds in nude mice increased epithelialization, compared to control, via ASC stimulated proliferation of human dermal fibroblasts by direct cell-cell contact and by paracrine activity [38,39]. ASC conditioned media was shown to promote increased proliferation and survival of HaCaT cells (immortalized keratinocytes) and primary dermal fibroblasts and to increase migration of HaCaT cells in a scratch assay [40].

Overall, the data of the literature suggests that ASC are able to promote healing in both porcine and murine wound healing models and have a positive effect on re-epithelialization. While work has been done to apply ASC to cutaneous wounds to promote wound healing, thus far, it is a novel concept to deliver both ASC and EC to the site of injury via an acellular wound healing scaffold. Since Integra is already indicated for use in third degree burn wounds, investigating whether delivery of ASC or ASC+EC on Integra enhances its healing capabilities is a worthwhile study, and could set the stage for practical clinical applications in the near future.

1.6 Spray Delivery of Cells

As mentioned above, CEA is one approach to skin grafting, and involves taking the available (often small) areas of skin, removing a biopsy, and expanding the patient's cells into sheets of keratinocytes that can then be applied to the wound to provide coverage [14, 24]. However, the length of time required to prepare these sheets of keratinocytes (2-3 weeks), susceptibility to infection, and fragility has made them unsuitable in many cases [41–44]. As such, alternative mechanisms have been sought. The ReCell® spray device is a novel adaptation of the normal CEA application.

Instead of waiting days to weeks to deliver sheets of cells, keratinocytes are harvested from skin biopsies and sprayed over a much larger surface area. These cells which are isolated from the dermal-epidermal junction, are highly proliferative and thus assist with a faster healing rate [41].

This method of delivery may also be a useful way to apply other cell types to wounds.

2. HYPOTHESIS AND AIMS

Based on the literature review of the data previously published by our and other groups, and on our preliminary findings, we devised two hypotheses:

(1) Human ASC, by their paracrine activity, will promote revascularization of dermal matrices by the host, and accelerate wound closure (compared to control), when applied to full-thickness wounds.

and

(2) Co-seeding EC with ASC on dermal matrices will facilitate and enhance EC re-organization into vascular networks and thus improve graft revascularization and overall graft retention and wound closure.

In order to test the hypotheses, the following aims were developed:

1. To assess if ASC promote survival of EC and their reorganization into stable microvessel networks when these two cell types are co-seeded onto scaffolds.
2. To assess the response of keratinocytes to factors secreted by ASC and ASC+EC.
3. To determine whether transplantation of the dermal matrices pre-seeded with ASC or ASC+EC into acute murine full-thickness wounds, will result in efficient graft vascularization and promote wound closure, when compared with effect of intact grafts containing no cells.

3. METHODS

All procedures for collecting human tissues (umbilical cord and adipose tissue) were approved by the Indiana University School of Medicine Institutional Review Board.

3.1 Isolation and Culture of ASC, EC and Keratinocytes

Human adipose stromal cells (ASC) were isolated from human subcutaneous adipose tissue samples obtained from liposuction procedures. Briefly, samples were digested in 1 mg/ml of collagenase type I solution (Worthington Biochemical, Lakewood, NJ) under agitation for one hour at 37°C, and then centrifuged at 300g for eight minutes to separate the stromal cell fraction (pellet) from adipocytes. The pellets were filtered through 250 μm Nitex filters (Sefar America Inc., Kansas City, MO) and treated with red cell lysis buffer (154mM NH_4Cl, 10mM $KHCO_3$, and 0.1mM EDTA). The final pellet, also called SVF, was re-suspended and cultured in EGM-2mv (Lonza, Walkersville, MD). Media was changed after first 24 hours, and then every 3-4 days. Monolayers of ASC were passaged when 60-80% confluent and used at passages 3-6. Purity of ASC samples from endothelial cells was confirmed by staining of ASC monolayers with anti-CD31 antibodies.

Cord blood-derived endothelial cells (EC) were isolated from the umbilical cord vein blood of healthy newborns (38-40 weeks gestational age). Mononuclear cells were isolated from blood samples by gradient centrifugation through Histopaque 1077 (ICN, Costa Mesa, CA), followed by culturing in EGM-2/10% FBS (Lonza) media in six well tissue culture plates (50×10^6 cells/well) pre-coated with 50 μg/ml of type I rat tail collagen (BD Biosciences, San Diego, CA). The culture medium was changed daily for seven days, and then every other day until first passage. Confluent EC were re-plated into flasks coated with rat tail collagen type I, and cultured in

EGM-2/10%FBS medium. Cells were passaged after becoming 90% confluent and used at passages 6-13.

Neonatal Normal Human Epidermal Keratinocytes (NHEK) were obtained from Lonza and grown in KGM-Gold media (Lonza). Cells were passaged after becoming 75%-90% confluent and used at passages 3-6.

ASC ($60 \times 10^3/cm^2$) and EC ($10 \times 10^3/cm^2$) were pre-mixed and plated on culture plastic. Cells were cultured in DMEM/F12 supplemented with 1% BSA for six days, with media change at day three.

3.2 Transduction of ASC and EC with GFP and DsRed Encoding Lentiviral Constructs

ASC were plated in T-25 flasks at a density of 1×10^4 cells/cm^2 in EGM-2mv and EC in T-25 flasks at a density of 2×10^4 cells/cm^2 in EGM-2/10% FBS. In three hours post plating, media on cell monolayers were exchanged for fresh one supplemented with 8 μg/ml of polybrene and 10% (by volume) of pCSCGW-DsRed2 lentiviral stock solution or 2% (by volume) of pCSCGW-EGFP lentiviral stock solution. The next day, the transduction solution was removed and replaced with fresh culture media. The cells were expanded and then sorted using FACS Aria Sorter. Cells with extremely high and very low expressions of fluorescent protein were discarded, and cells with a median fluorescent protein expression were collected for expansion. Non-transduced ASC and EC were used during sorting procedure to establish cutoff for autofluorescence. After sorting, cells were replated for expansion.

3.3 EC, ASC and ASC+EC Cultivation on Integra and Alloderm Scaffolds

GFP-expressing ASC and DsRed-expressing EC were seeded onto 1 cm^2 rectangular pieces of Integra (Integra LifeSciences, Plainsboro, NJ) and Alloderm (Lifecell Corporation, Branchburg, NJ) in EBM-2/5%FBS/1%penicillin/streptomycin. Inte-

gra is a bovine-derived, collagen-based matrix with a silicone backing. The matrix serves as the "dermal" side and the silicone backing serves as the "epidermal" side. The silicone backing prevents moisture loss and provides a barrier to pathogens. Alloderm is decellularized, freeze-dried human dermis. It also has a shiny, smooth, white dermal side and a rough, dull, buff-colored basement membrane side. In both scaffolds, cells were seeded on the dermal side.

In the experiment there were three groups with n = 3 in each one: (1) ASC alone (10^5 cells/cm^2, P5); EC alone (10^5 cells/cm^2, P10); (3) co-culture with 10^5 cells/cm^2 ASC + 10^5 cells/cm^2 EC.

Integra and Alloderm were cut to fit into the chambers of 8-well glass slides (BD Biosciences, MA). Cells were seeded on scaffolds in 100 μl of EBM-2/5%FBS/ 1% penicillin/streptomycin, and allowed to attach overnight. The next day, the scaffolds were transferred to non tissue culture treated 24-well plates (Corning Inc, NY) in media, with side on which cells were seeded, facing up. They were maintained in these 24-well plates for the duration of the experiment.

To monitor cell survival and their reorganization into microvessels, images of mono- and co-cultures on Alloderm and Integra were taken every day with a Nikon Eclipse Ti microscope with channels appropriate for detection of GFP and DsRed fluorescent proteins.

3.4 Generation of Conditioned Media By ASC and ASC+EC Cultures When Plated on Tissue Culture Plastic

To generate conditioned media from ASC and ASC+EC co-cultures, three different ASC samples at passages 2 and 3 and one sample of EC at passage 10 were used. ASC alone from each donor (6×10^4 cells/cm^2) and ASC + EC (6×10^4 cells/cm^2 of ASC and 10^4 cells/cm^2 of EC) were seeded into T-25 flasks in 4.5 ml of DMEM/F12/5% FBS. Cells were allowed to attach for a few hours and then the media was exchanged for DMEM/F12/1%BSA for overnight incubation. The next

day, media was replaced with fresh DMEM/F12/1%BSA and cells were incubated for 72 hours. At the end of the incubation period, the media was collected, spun down to remove debris and dead/floating cells, aliquoted, and stored at $-80°C$. The outcome was six different conditioned media samples (three from ASC alone and three from ASC+EC, each from three different ASC donors). These media were used to test keratinocyte survival and migration.

3.5 Generation of Conditioned Media By ASC and ASC+EC When Cultured On Integra and Alloderm

ASC and EC were seeded onto 1 cm^2 pieces of Integra and Alloderm in EBM-2/5%FBS/1%penicillin/streptomycin. There were two groups: ASC alone ($10^5/cm^2$) and co-culture of ASC ($10^5/cm^2$) with EC ($10^5/cm^2$). Three different ASC samples were used, as described above. The outcome was six different sets of conditioned media (three from ASC alone and three from the same three ASC samples, each combined with EC from the same donor). Conditioned media was collected every day, spun down to remove cellular debris, and frozen for future evaluation.

3.6 Evaluation of Effects of ASC and ASC+EC Conditioned Media on Keratinocyte Survival

Keratinocytes were seeded in KGM-Gold growth medium at 25×10^3 cells/cm^2 into 24-well plates. The next day, the medium was switched to DMEM/F12/1%BSA and cells were incubated overnight. After that, cells were exposed to ASC or ASC+EC conditioned media (diluted 1:1 with fresh DMEM/F12/1% BSA) for six days with a media change at day three. The control medium consisted of DMEM/F12/1%BSA. After six days, the keratinocytes were fixed in cold methanol and stained with eosin. From each well, nine images were taken at 20x magnification. The areas covered by cells in each image were quantified using Nikon Elements software (Nikon, Melville, NY).

3.7 Evaluation of Effects of ASC and ASC+EC Conditioned Media on Keratinocyte Migration

Strips of parafilm were cut, rinsed in 70% ethanol, allowed to dry and then pressed to the bottom of wells of a 24 well plate, along the center. Keratinocytes were seeded in their growth medium over the parafilm strips at 15×10^4 cells/cm^2 overnight, after which the growth medium was replaced with DMEM/F12/1%BSA for 24 hour incubation. The next day, the strips of parafilm were removed, leaving a thin cell-free gap. ASC or ASC+EC conditioned media was mixed 1:1 with fresh DMEM/F12/1%BSA and applied to cells (n=4). Gaps formed after parafilm strip removal were photographed; the cells were incubated for 48 hours in the conditioned media, then fixed with cold methanol and the gaps photographed again. Control wells were incubated with DMEM/F12/1%BSA. Image J (NIH) was used to trace and measure the change in the gap area from t = 0 to t = 48 hrs.

3.8 Preparation of Integra Scaffold For Implantation

Integra scaffolds were cut into circular discs using an 8 mm biopsy punch tool (Acuderm, Fort Lauderdale, FL). With a thickness of 0.1 cm and radius of 0.4 cm, the total volume of each scaffold was calculated as: $0.05\ cm^3$. Non-transduced ASC and DsRed expressing EC were seeded onto the dermal side of the scaffolds at a concentration of 10×10^6 cells/cm^3 (500,000 cells/scaffold). Cells were seeded onto the scaffold the day before implantation. Integra scaffolds were seeded with: (1) ASC alone (50×10^4 cells/scaffold), (2) ASC+EC (25×10^4 ASC + 25×10^4 EC). Control consisted of Integra scaffolds (no cells seeded) soaked in DMEM/F12/1%BSA.

3.9 Mouse Full-Thickness Wound Model

Animal studies were approved by the Institutional Animal Care and Use Committee of Indiana University. In the model, NOD/scid/IL2Rgnull (NSG) mice were used.

Wounds were made down thru the panniculus carnosus with an Acuderm biopsy punch tool (Acuderm) and then cut out using an Iris scissor. Integra scaffolds were prepared and incubated overnight as described above. The next day, they were pushed through the wound window and positioned cell side up at the center of the wound window as much as possible. Tegaderm (3M, St. Paul, MN) was used to cover the wounds to keep them from drying out and to protect them from bacterial contamination. It also served as a splint to inhibit wound contraction. To reinforce the Tegaderm and prevent the mice from removing it and disturbing the wounds, mice were bandaged with Vetrap (3M, St. Paul, MN). Mice were checked daily to ensure that the bandages stayed in place. If necessary, mouse was rebandaged. Mice were kept under 1.5% isoflurane gas anesthesia during surgery, during scaffold implantation, and each time wounds were imaged.

3.10 Power Analysis On Pilot Mouse Study Data

A pilot experiment was performed in anticipation of the full animal study. Data from the pilot was used to generate a Monte Carlo based power analysis. In the pilot study: (1) 5 male NSG mice were used, (2) Silicone backing was removed from the Integra before placing in wound. (3) A 4 mm Acuderm biopsy punch tool was used to make the wounds, (4) Experiment was stopped at Day 11, and (4) No cells were seeded on scaffold (all controls). The 5 NSG mice were wounded as described above. Discs of Integra scaffold (without cells) with the silicone backing removed, were placed in the wound windows. The wound closure rate in these control mice was used to perform a power estimation. The power estimation helped determine the number of wounds needed in each treatment group and control, to detect a statistical difference between control and treatment groups.

The statistical model used to perform this analysis is outlined below. It was conducted by Michael G. Wilson, an independent biostatistician with Biostatistical

Communications, Inc :

$$Y(i,j,k) = \mu + [\beta(i) \times trtgrp(i) \times day] + animal(i,j) + \epsilon(i,j,k) \qquad (3.1)$$

Where:

i = 1, 2, or 3

j = 1, 2, , n

k = 1 or 2 (right or left)

n = number of animals per treatment group

μ = the overall intercept (mean)

trtgrp (i) denotes an indicator variable for the ith treatment

day is the numeric day of the measurement (one degree of freedom)

animal (i,j) is random variable and is distributed iid N(0, σ^2(for animal))

β(i) denotes the slope of the ith treatment

ϵ (i,j,k) is random error and is distributed iid N(0, σ^2 (for error))

animal (i,j) and epsilon (i,j,k) are independent

The rate of healing at day 11 was used in the model (pilot). At this time point, the average wound area was 7 mm^2, and the slope was -1.27 mm^2/day. Since no treatment groups were analyzed in the pilot, their slopes were estimated for the model. The assumption was made that ASC+EC would have a steeper slope than ASC alone. ASC alone would have a steeper slope than the control. With that in mind, the wound size for the ASC treatment group at Day 11 was estimated to be about 5 mm^2, which gave a slope of -1.45 mm^2/day. The wound size for the ASC+EC treatment group was estimated to be about 3 mm^2 at day 11, giving a slope of -1.64 mm^2/day.

The power was estimated using a Monte Carlo simulation using the control slope, the estimated treatment slopes, and the correlational time structure (Toeplitz correlation). Toeplitz refers to a matrix where every descending diagonal from left to

right is constant. The study was simulated 10,000 times and then analyzed using the mixed linear model outlined above.

3.11 Animal Study

Nine male and nine female NSG mice that were six weeks old were used in this study. Scaffolds were prepared with ASC or ASC+EC, and wounds made as described above, except that: (1) Silicone backing remained intact and was not removed from the Integra before placing in wound. (2) A 3 mm Acuderm biopsy punch tool was used to make the wounds, and (3) Experiment was stopped at Day 20. With silicone layer still intact, cellular migration into scaffold from below the scaffold was inhibited. At day 0, 7, 10 and 14, bandages were removed and images of the mouse wounds were taken using a digital camera. A ruler was placed in each of the images to serve as a scale. Images were analyzed using Image J to measure wound areas. At day 20, mice were sacrificed and implants were harvested for histological analysis.

3.12 Statistical Analysis of Mouse Study

An ANCOVA Model with Main Effects with Multiplicative interaction was the model used to test the primary hypothesis. The model, as outlined below, was built by Michael G. Wilson. While the ANCOVA model used here is different than the one used in the power estimate, the two models give similar conclusions (data not shown) and this given model has the advantage of fitting the data better and being less controversial, by generating fewer statistical comments. This was confirmed by the corrected Akaike information criterion (AICC) numbers (578.5 vs. 586.7). These numbers define the relative quality of a statistical model, and their difference is used to determine the relative likelihood of two models, with a higher difference resulting in a higher likelihood that the model with the smaller number fits the data best [45].

$$Y(i,j,k) = \mu + \beta 1(i) \times trtgrp(i) + \beta 2 \times day + [\beta 3(i) \times trtgrp(i) \times day] + animal(i,j) + \epsilon(i,j,k) \quad (3.2)$$

Where:

i = 1, 2, or 3

j = 1, 2, , n

k = 1 or 2 (right or left)

n = number of animals per treatment group

μ = the overall intercept (mean)

trtgrp (i) denotes an indicator variable for the ith treatment

day is the numeric day of the measurement (one degree of freedom)

animal (i,j) is random variable and is distributed iid N(0, σ^2 (for animal))

$\beta 1$ (i) denotes the effect of the ith treatment

$\beta 2$ denotes the effect due to day

$\beta 3$ (i) denotes the slope of the ith treatment

ϵ (i,j,k) is random error and is distributed iid N(0, σ^2 (for error))

animal (i,j) and epsilon (i,j,k) are independent

3.13 Immunohistochemical Analysis of Implanted Grafts

At 20 days, mice were sacrificed, and the scaffolds were removed with any attached tissue. The Integra scaffolds were fixed in 10% formalin solution (Fisher Scientific, Kalamazoo, MI), cut in half, paraffin embedded, and then sectioned. Slides were Hematoxylin & Eosin (H&E) stained and examined for RBC containing vessels in the scaffold. ASC+EC sections were also stained with mouse anti-human CD31 IgG (Dako, Carpinteria, CA) to detect vessels formed by donor endothelial cells. Briefly, tissue sections were incubated for 15 minutes with mouse anti-human CD31 (primary). Next, tissue was incubated with a labeled polymer for 10 minutes. Finally, DAB development was done for 10 minutes.

3.14 Pilot experiments for future direction of project

3.14.1 Seeding keratinocytes with ASC and ASC+EC on Integra Scaffold

Keratinocytes were seeded alone, or with ASC, or with ASC+EC on disks (r = 4mm) of Integra scaffold in DMEM/F12/1%BSA. For this experiment, GFP-ASC and DsRed-EC were used. Keratinocytes were labeled with DiD (Molecular Probes, Eugene, OR) following the manufacturer protocol. Keratinocyte alone group was seeded at 5×10^4 cells/scaffold. 50×10^4 ASC were mixed with 5×10^4 keratinocytes before seeding on scaffold for ASC+keratinocyte case. ASC+EC (25×10^4 cells each) were mixed with 5×10^4 keratinocytes before seeding on Integra. Images were taken at Day 2.

3.14.2 Spraying Cells With ReCell®

To test the feasibility of spraying ASC, EC and keratinocytes in anticipation of a clinical study, keratinocytes, GFP-ASC and DsRed-EC were sprayed into a petri dish using a ReCell® Spray-On Skin kit (Avita Medical, CA), provided by Dr. R. Sood. The petri dish was covered with a thin layer of DMEM/F12, 5% FBS. Feasibility of successful delivery of ASC, EC, and keratinocytes via spray technology was considered by comparing to the dripped case. Cell suspensions GFP-ASC+DsRed-EC+unlabeled keratinocyte (7×10^4 each) were mixed, taken up with 5ml syringes and either dripped from the syringe or sprayed by attaching the nozzle to the tip of the syringe. After either spraying or dripping, cells were transferred to a 6 well plate. Fifteen images were taken of each well at 10x using a Nikon Eclipse Ti camera. The next day, cells were counted and number/unit area determined.

Freshly prepared SVF sample was resuspended in EGM2-mv. To prepare the SVF for spraying, it was filtered again using a 40 μm filter. The cell suspension was taken up by a syringe and sprayed with a ReCell® spray nozzle, into a thin layer of EBM-2/5%FBS in a petri dish. The cells were then transferred to a 48 well-plate.

After six days, the SVF was fixed and stained for Lectin to detect vessel formation. Briefly, cells were incubated with biotin labeled lectin (Vector labs, CA) for 1 hour, and streptavidin elexa 488 (Vector labs, CA) for 30 minutes.

4. RESULTS

4.1 ASC Promote Survival of EC and Stabilize Microvascular Networks On Dermal Matrices

In order to determine if ASC stabilization of vascular endothelial networks (as observed in collagen plugs and on tissue culture plastic by our lab [27, 32]) occurred when the cells were seeded on dermal matrices, ASC alone, EC alone, or ASC+EC cell mixture were seeded on rectangular pieces of Integra and Alloderm as described in the Methods.

EC, when seeded alone onto dermal matrices, showed little survival after 7 days (Figures 4.1 and 4.2). ASC, however, not only survived on Integra and Alloderm after 7 days, but also promoted survival of EC and the stabilization of vascular networks as was previously observed. Merfeld-Clauss, et al. have shown evidence that ASC, via paracrine mechanisms and cell-to-cell contact, stabilize the formation of microvessel networks formed by EC [32]. We hypothesize that this is the likely mechanism of microvessel formation on Integra and Alloderm.

Interestingly, it is observed that the microvessels formed on Alloderm seemed to form on the surface of the scaffold, indicating that cellular penetration into Alloderm was minimal. At the same time, microvessels formed on Integra appeared to have more 3D organization, suggesting deeper penetration into the scaffold. Confocal microscopy analysis was done to support this prior observation and to demonstrate 3D organization of the EC in the matrix (see Figure 4.3).

As has been discussed already, timely revascularization is critical for graft integration and overall patient recovery [26]. Thus, the rate of network formation by ASC+EC co-cultures is of interest, as this will affect the rate of healing and of graft integration. Figures 4.4 and 4.5 show the dynamics of EC organization into vascular

networks during the 7 day period after plating on Integra and Alloderm, respectively. By day 3 networks begin to form and by day 5, the vascular network is mostly organized.

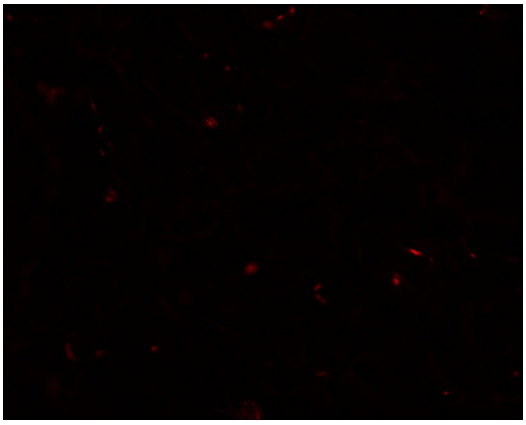

(a) EC alone on Integra.

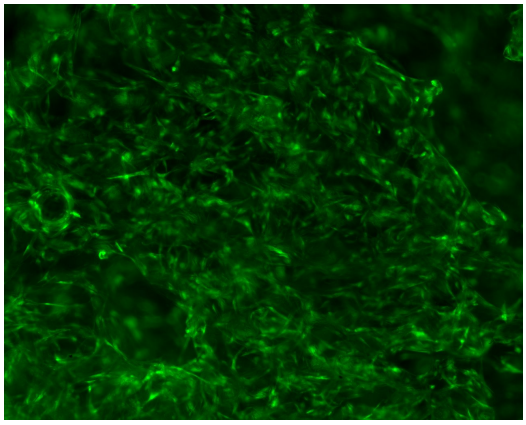

(b) ASC alone on Integra.

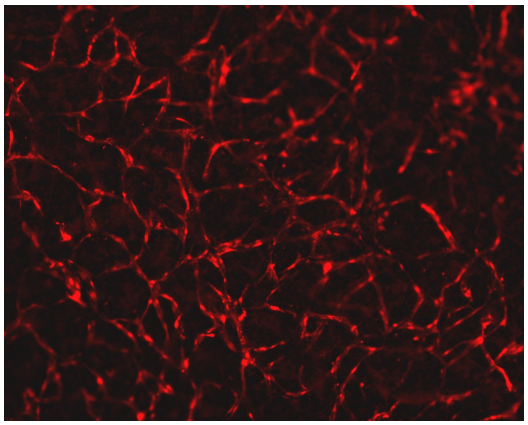

(c) ASC+EC on Integra.

Fig. 4.1. ASC, EC, and ASC+EC survival on Integra. Representative images of GFP-ASC (green) and DsRed-EC (red) seeded (a, b) alone or in (c) mixture (1:1) onto Integra taken at day seven post plating (n = 5).

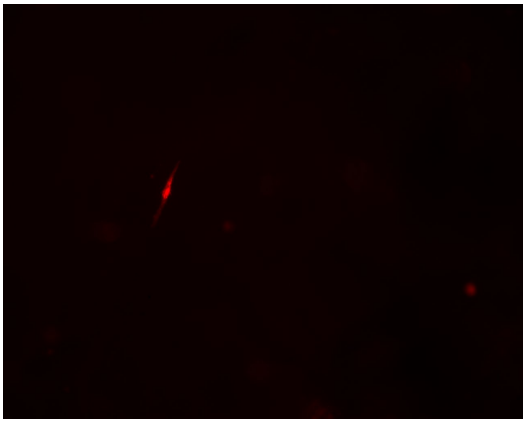

(a) EC alone on Alloderm.

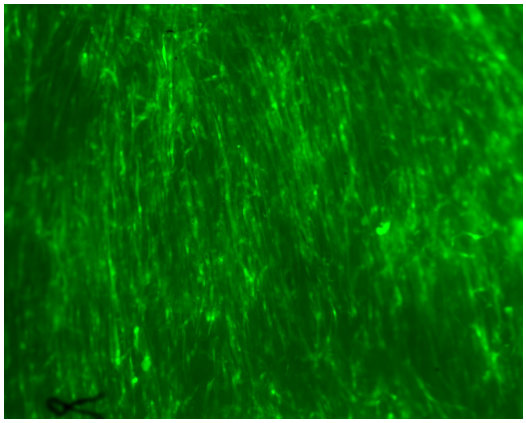

(b) ASC alone on Alloderm.

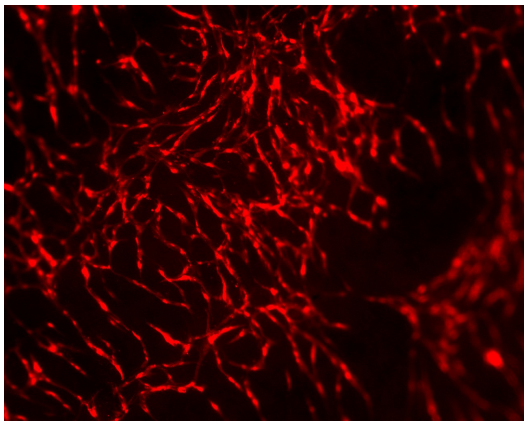

(c) ASC+EC on Alloderm.

Fig. 4.2. ASC, EC, and ASC+EC survival on Alloderm. Representative images of GFP-ASC (green) and DsRed-EC (red) seeded (a, b) alone or in (c) mixture (1:1) onto Alloderm taken at day seven post plating (n = 5).

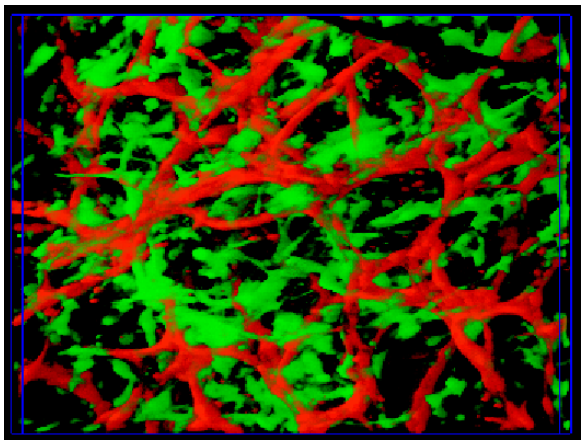

(a) View 1.

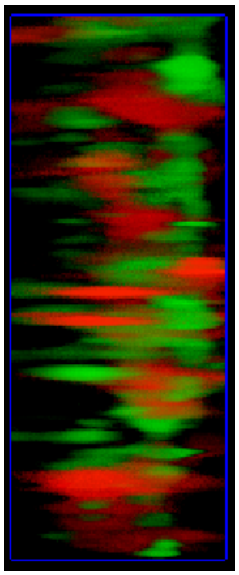

(b) View 2.

Fig. 4.3. Snapshots from confocal based movie clip showing (a) 3D organization of ASC (green) and EC microvessels (red) on Integra and (b) 100 μm depth of section.

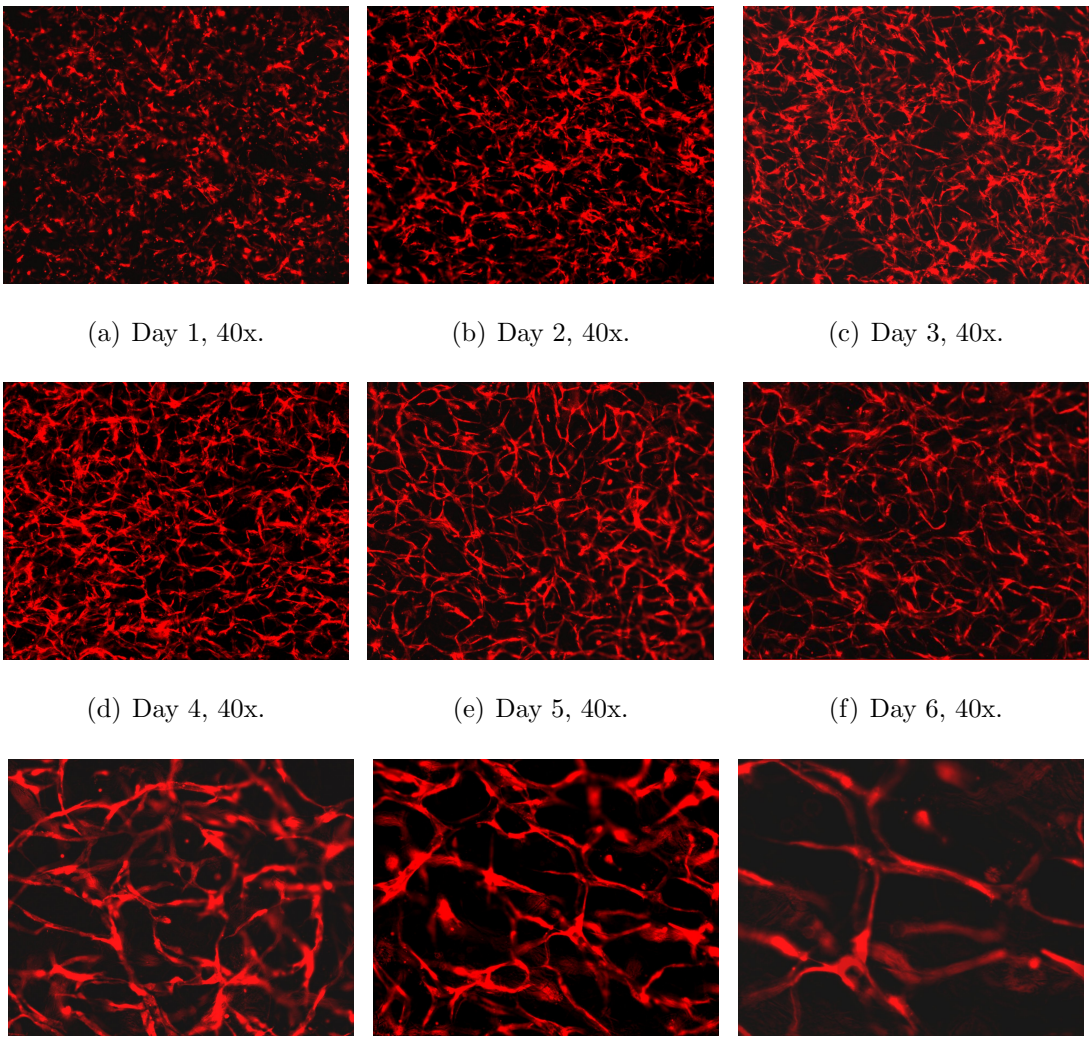

(a) Day 1, 40x. (b) Day 2, 40x. (c) Day 3, 40x.

(d) Day 4, 40x. (e) Day 5, 40x. (f) Day 6, 40x.

(g) Day 4, 100x. (h) Day 7, 100x. (i) Day 7, 200x.

Fig. 4.4. Dynamics of EC organization into microvessels on Integra, when co-plated with ASC. We plated mixture of DsRed-EC and GFP-ASC (1:1). Pictures were taken daily for 7 days using a Nikon Eclipse Ti with appropriate channel for DsRed fluorescent protein (n = 3). (a)-(f) Day 1-Day 6, 40x. (g) Day 4, 100x. (h) Day 7, 100x. (i) Day 7, 200x

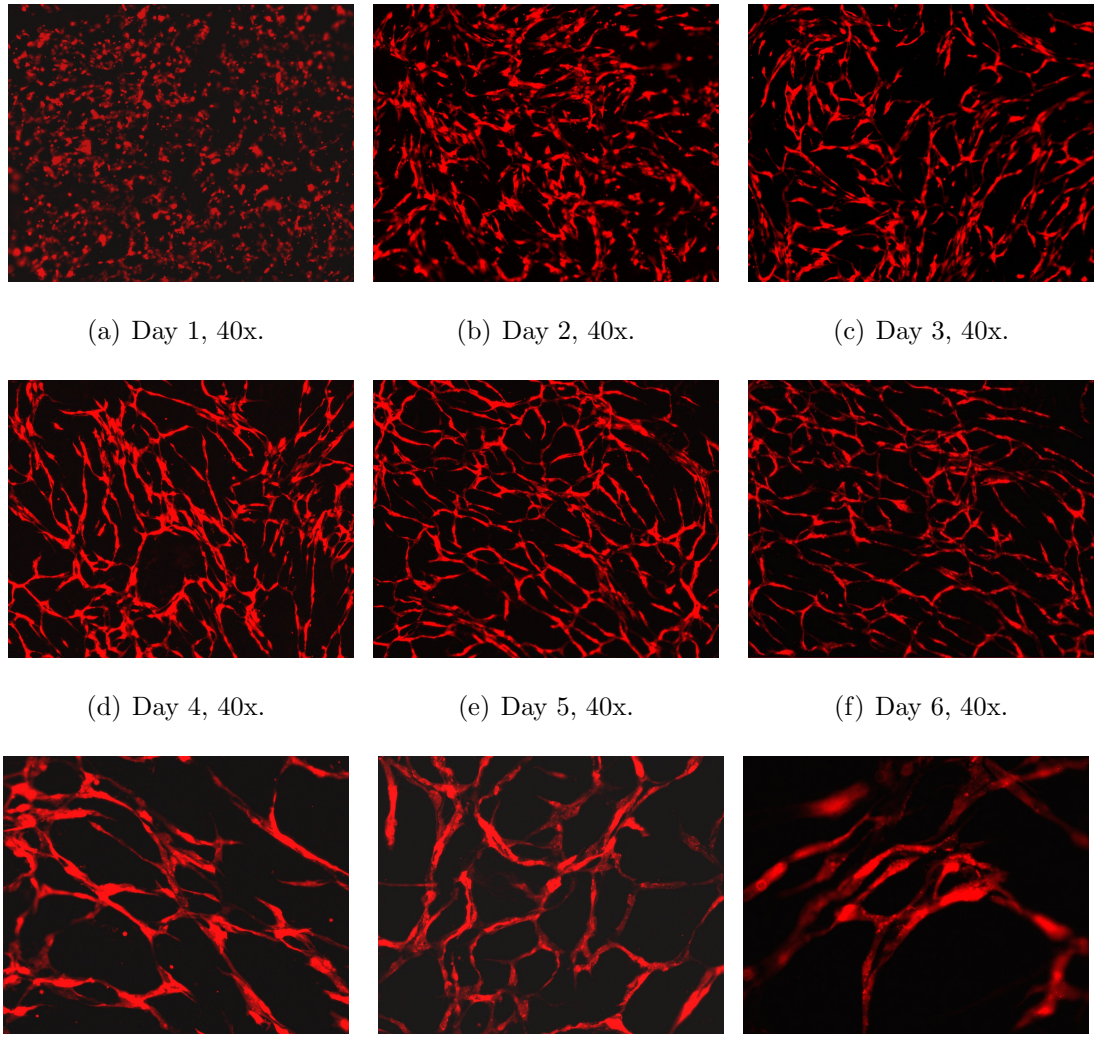

(a) Day 1, 40x. (b) Day 2, 40x. (c) Day 3, 40x.

(d) Day 4, 40x. (e) Day 5, 40x. (f) Day 6, 40x.

(g) Day 4, 100x. (h) Day 7, 100x. (i) Day 7, 200x.

Fig. 4.5. Dynamics of EC organization into microvessels on Alloderm, when co-plated with ASC. We plated mixture of DsRed-EC and GFP-ASC (1:1). Pictures were taken daily for 7 days using a Nikon Eclipse Ti with appropriate channel for DsRed fluorescent protein (n = 3). (a)-(f) Day 1-Day 6, 40x. (g) Day 4, 100x. (h) Day 7, 100x. (i) Day 7, 200x

4.2 ASC and ASC+EC Conditioned Media (CM) Promotes Keratinocyte Survival

Other studies have shown that ASC secrete paracrine factors that promote cell survival [31, 32]. Moreover, in this study we have shown their impact on EC survival and the stabilization of vascular networks (Figures 4.1 and 4.2). Factors secreted by ASC are also known to improve healing in cutaneous wounds in various animal disease models [34, 37–39]. With this in mind, we wanted to look at the effect of ASC secretions on keratinocyte survival.

To investigate this, 72 hour ASC and ASC+EC conditioned media was collected as described in the Methods section. The conditioned media was applied to sub-confluent cultures of normal human epidermal keratinocytes. As shown in Figure 4.6(a), both of these medias were able to increase survival of primary human keratinocytes by about 2.5 times compared to control. There is always a concern with variability in behavior of the cells obtained from different donors. However, our experiment has shown that the media collected from three ASC samples has a significant positive effect, with no differences observed between the samples (Figure 4.6(b)).

4.3 ASC and ASC+EC CM Promotes Migration Of Keratinocytes In Cell In-Growth Assay

Noting ASC ability to promote faster healing of cutaneous wounds, we wanted to investigate the effect of factors secreted by ASC on keratinocyte migration (as it may be a possible mechanism of the enhanced wound closure previously observed [34, 37–39]). To evaluate this effect, we used a wound closure assay as explained in the methods section. After creating the gap in keratinocyte monolayer, the cells were incubated in 50% of 72-hour ASC or ASC+EC conditioned media, diluted with fresh DMEM/F12/1%BSA for 48 hours. The results (Figure 4.7(a)) indicated that the cell migration rate into the gap was increased by 75% in response to both treatments compared to control. This suggests that paracrine secretions may play a major role

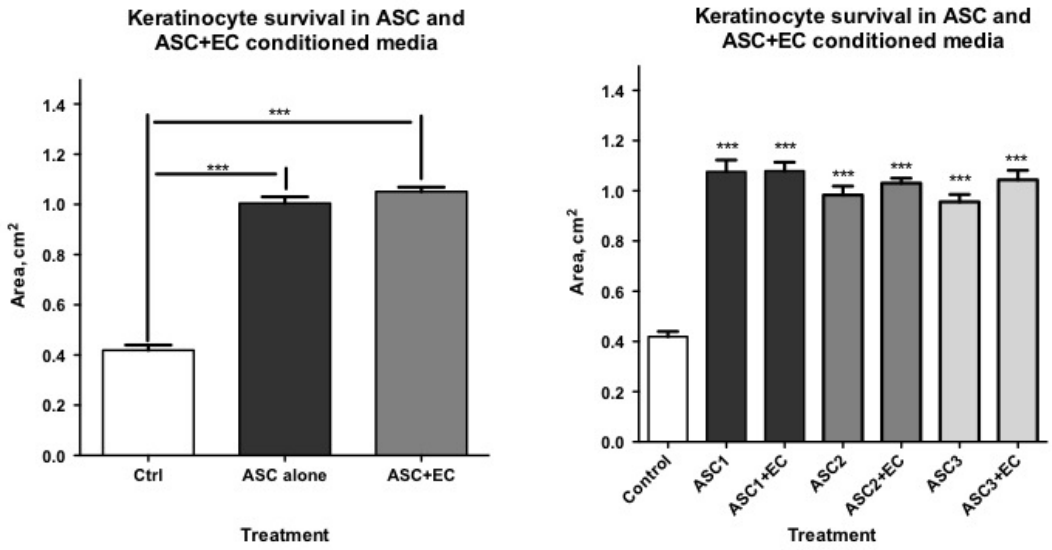

(a) Three ASC donor results combined.

(b) ASC from three different donors.

Fig. 4.6. Media conditioned by ASC & ASC+EC promote survival of keratinocytes. Keratinocytes were seeded at 25 x 10^3 cells/cm^2 into 24 well plates. They were incubated in 50% ASC or ASC+EC conditioned media (diluted with fresh DMEM/F12/1% BSA) for 6 days. There were three different donor ASC samples tested, with an n of four in each ASC and ASC+EC pair. After 6 days, the keratinocytes were fixed in cold methanol and stained with eosin. From each well, nine images were taken at 20x magnification. The area covered by cells in each image was quantified using Nikon Elements software. (a). All three donor ASC and ASC+EC results combined and compared to control. (*** , $p<0.001$) (b). Keratinocyte survival in response to each donor ASC and ASC+EC pair.

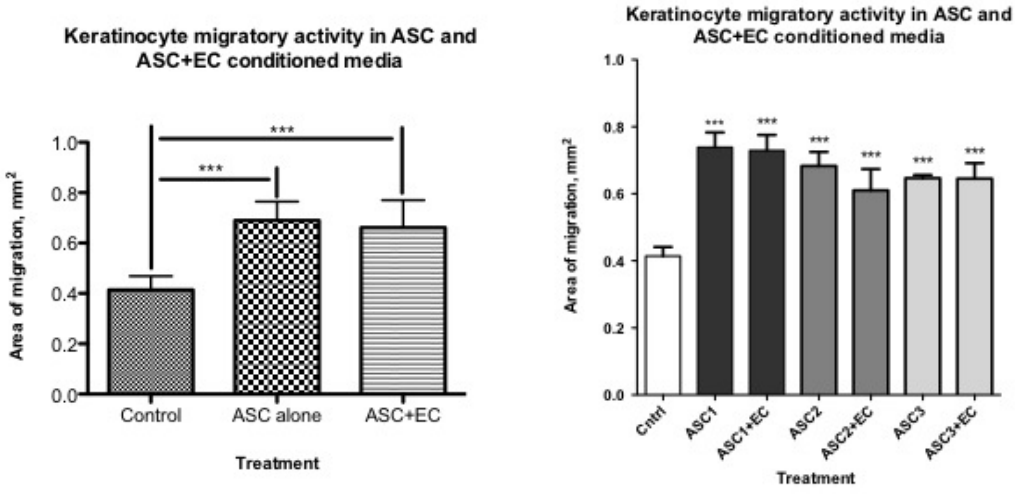

(a) Three ASC donor results combined.

(b) ASC from three different donors.

Fig. 4.7. Media conditioned by ASC and ASC+EC promotes migration of keratinocytes. Gaps formed in the midline of the wells after parafilm strip removal, were photographed. At the end of 48 hours, the cells were fixed with cold methanol and photographed again. There were three different donor ASC samples tested, with an n of four in each ASC and ASC+EC pair. Image J (NIH) was used to trace and measure the change in the gap area from t = 0 to t = 48 hrs. (a). All three donor ASC and ASC+EC results combined and compared to control. (***, $p<0.001$ (b). Keratinocyte migration for each donor ASC and ASC+EC pair.

in ASC-stimulated wound closure by promoting cellular migration. Once again, our experiment has shown there is little variability between cells obtained from different donors (Figure 4.7(b)).

4.4 ASC and EC Secrete Pro-Angiogenic Growth Factors When Seeded On Dermal Matrices

ASC and ASC+EC conditioned media was shown to promote survival and migration of keratinocytes (Figures 4.6 and 4.7) and to promote survival and stabilization of vascular networks formed by EC on Integra and Alloderm (Figure 4.1 and 4.2). The conditioned media is composed of a variety of cytokines and growth factors. ELISA was performed to evaluate the presence of two known pro-angiogenic factors, HGF and VEGF, and to observe their daily accumulation in media conditioned by ASC and ASC+EC seeded on Integra and Alloderm. To normalize for any differences in cell-seeding number, values for day 1 were represented as 100%.

Analysis of conditioned media collected from Integra seeded with ASC+EC revealed that the level of VEGF was significantly higher at day 3 for the mixed condition compared to ASC alone (Figure 4.8(a)). However, after this, the VEGF secretion declines. By day 5 and day 6 there are significantly lower and lower amounts of VEGF accumulating in the media for the ASC+EC case compared to ASC alone. In Figure 4.8(b), on Alloderm, the ASC and ASC+EC group reaches a steady, consistent, daily accumulation of VEGF. The difference in VEGF accumulation on Alloderm vs. Integra may be due to differences in the properties of the two dermal matrices.

HGF, another pro-angiogenic factor, shows a sharp downward trend in daily accumulation for ASC and ASC+EC groups on Integra betwen Day 1 and Day 3. After this (Day 3-6), the secretion decline is a lot smaller (Figure 4.8(c)). Both ASC and ASC+EC groups on Alloderm show a steady downward trend in HGF accumulation (Figure 4.8(d)).

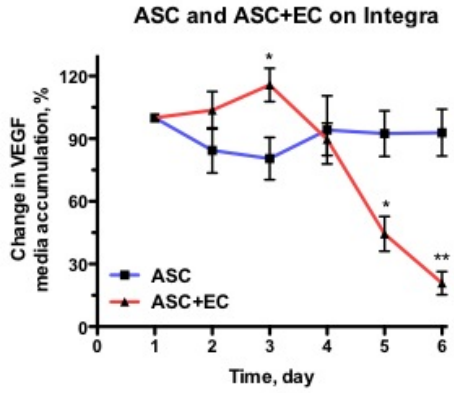

(a) VEGF accumulation on Integra.

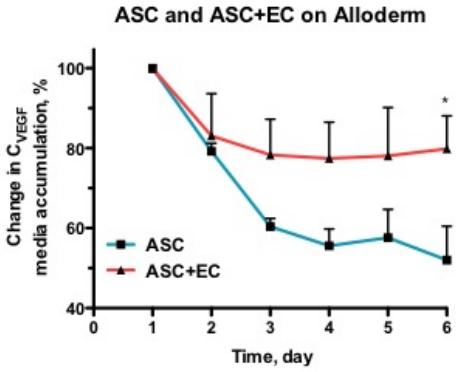

(b) VEGF accumulation on Alloderm.

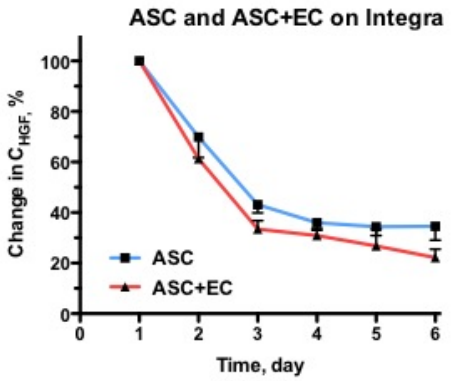

(c) HGF accumulation on Integra.

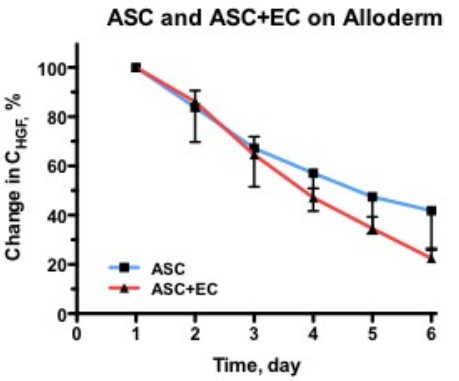

(d) HGF accumulation on Alloderm.

Fig. 4.8. VEGF and HGF Accumulation by ASC and ASC+EC seeded on Integra and Alloderm. ASC and ASC+EC (1:1) were seeded onto Integra and Alloderm as previously described. Media was collected every day and analyzed for accumulation of VEGF and HGF via ELISA. (n = 3). (a). Accumulation of VEGF in the media conditioned by ASC alone or by ASC+EC cell mixture when seeded onto Integra. (b). Accumulation of VEGF in the media conditioned by ASC alone or by ASC+EC cell mixture when seeded onto Alloderm. (c). Accumulation of HGF in the media conditioned by ASC alone or by ASC+EC cell mixture when seeded onto Integra. (d). Accumulation of HGF in the media conditioned by ASC alone or by ASC+EC cell mixture when seeded onto Alloderm.

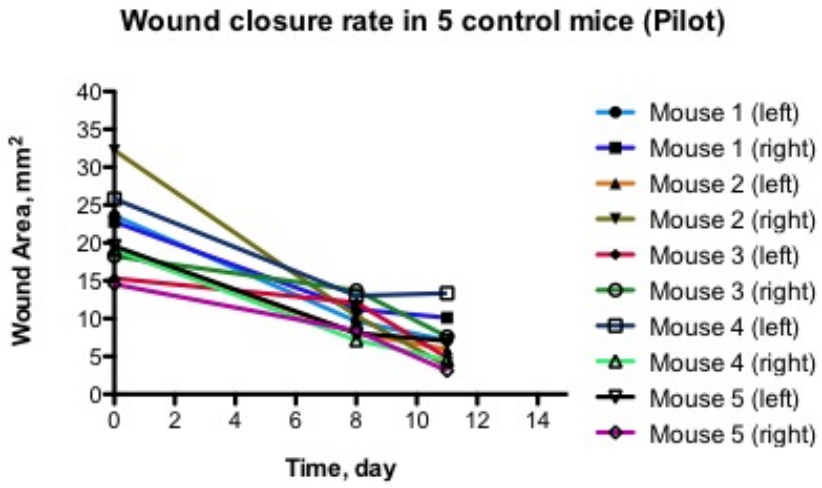

Fig. 4.9. Wound closure trend in five control mice. The average rate of healing for all 10 wounds at day 11 was calculated (-1.27 mm^2/day) and used in the model. Bilateral wounds were made down thru the panniculus carnosus with a 4 mm Acuderm biopsy punch tool on the dorsum of 5 NSG mice, and then cut out using an Iris scissor. Integra with the silicone backing removed was placed in wound windown. Wounds were covered with Tegaderm and bandaged with Vetrap. Images of the mouse wounds were taken at days 0, 8, and 11 using a digital camera, and Image J was used to measure wound areas based on the images.

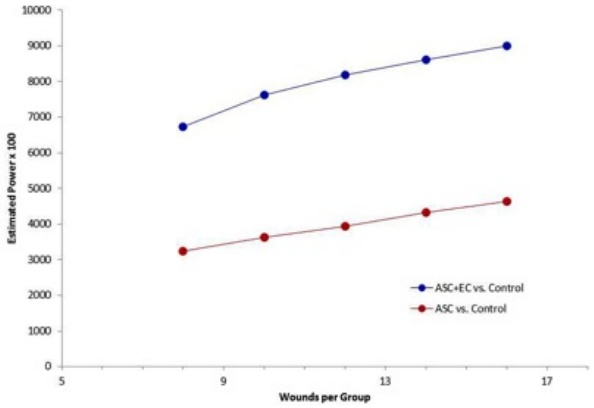

Fig. 4.10. Estimated Power to detect differences in wound area for each treatment animal. In the model, the control ASC+EC group was estimated to have the highest power overall with 12 wounds/group giving a power of 80% compared to 40% for ASC alone group. The power was estimated using a Monte Carlo simulation using the control slope, the estimated treatment slopes, and the correlational time structure (Toeplitz correlation). Rate of healing at Day 11 was used in the model outlined in Equation 3.1. In pilot, average rate of healing at day 11 for the controls was -1.27 mm^2/day. Based on our estimation, the ASC group was modeled at -1.45 mm^2/day and the ASC+EC at -1.64 mm^2/day.

4.5 Pilot Study Results Used To Generate Power Analysis For In Vivo Experimental Design

With supporting in vitro work, the next step was to observe how ASC and ASC+EC would influence healing in murine full-thickness wounds. Using the results from a pilot experiment (Figure 4.9) which investigated the wound closure rate in 5 mice (2 wounds each) treated with Integra scaffold alone (no cell treatment), a power analysis was performed. The goal was to determine a reasonable n for the experimental study. The power analysis was estimated using a Monte Carlo simulation (see Methods). The average rate of healing for all 10 wounds at day 11 was calculated (-1.27 mm^2/day) and used in the model. The rate of healing for ASC treatment was estimated to improve by 15% more than control, at -1.45 mm^2/day and the ASC+EC treatment was estimated to improve by 30% at -1.64 mm^2/day. The ASC and ASC+EC treatment values were purely estimates based on speculation and were not scientifically derived. With this in mind, we understand the limitations of the model, but it provided a basis for informing the n of the experimental design in a hypothetical case. Based on the experimental control slopes, the estimated treatment slopes, and the correlational time structure (Toeplitz correlation) the graph for the power estimate is seen in Figure 4.10. In the experimental design, we chose to use 12 wounds per treatment, which gave a power estimate of around 40% for the ASC group vs. Control and around 80% for the ASC+EC group vs. Control.

4.6 Implantation Of Integra Pre-Seeded With ASC+EC Improves Rate Of Wound Closure Compared To Integra Alone, In Cutaneous Full-Thickness Wound Model

The pilot test served as the foundation of the full animal study. The experimental design of the study is described in the Methods. In our current model, we began with a total of 6 mice per group, which, with 2 wounds per mouse gave us 12 wounds per mouse. However, due to a number of reasons which are listed, several wounds had

to be discounted or could only be used for one or two time points. Final n used for wound closure analysis at each time point:

Control: Day 7 (6), Day 10 (5), Day 14 (4) ASC: Day 7 (8), Day 10 (4), Day 14 (6) ASC-EC: Day 7 (6), Day 10 (4), Day 14 (5)

Wounds had to be excluded for the following reasons:

1. Wound contamination. White or greenish-yellow pus developed on a number of wounds and reaction inhibited wound closure. The cause is unsure. In some cases, a yellowish substance developed on the wounds and initially it was thought this could be contamination, but the wounds progressed and closed as expected, so it was ruled to likely be a fibrin exudate that is often released from wounds.

2. Scaffold not found in mouse on day of sacrifice or found in a different location than the wound window. There were several times that the mice removed their bandages and tegaderm and had to be rebandaged. These are points where the Integra scaffolds could have been removed.

3. Scaffold folded up in wound window, holding wound open.

4. Tegaderm not staying attached to wound under bandage.

5. One mouse died under anesthesia on Day 7 and three on Day 14.

However, even with the loss of so many data points, sufficient data was collected to detect a statistically faster rate of wound closure for the ASC+EC treatment group (Figure 4.11(a) using the ANCOVA statistical model (see Equation 3.2 in Methods). However, ASC alone wound closure rate was not significantly different than control, though it was faster (Figure 4.11(b).

The slopes for the control and treatment groups were approximated using best linear unbiased estimates (BLUE). Based on BLUE analysis, the slopes were calculated to be -0.48 mm^2/day for control, -0.93 mm^2/day for ASC treatment group and -1.03 mm^2/day for ASC+EC treatment group. The BLUE for the difference between the

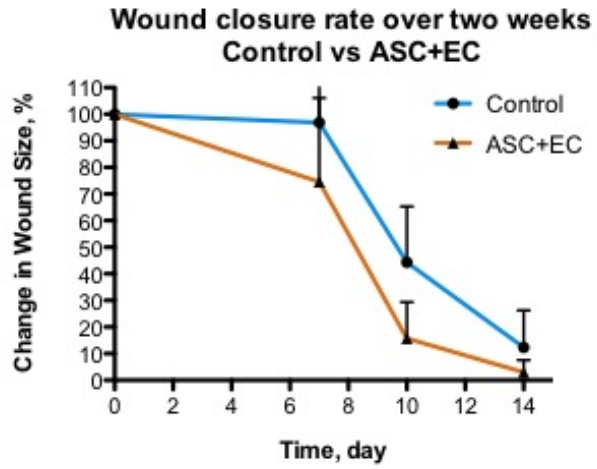

(a) Wound Closure Rate in ASC + EC vs. Control.

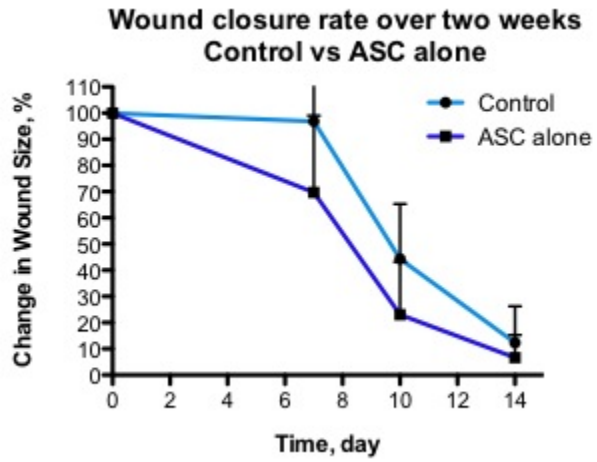

(b) Wound Closure Rate in ASC alone treatment vs. Control.

Fig. 4.11. Wound closure rate of murine, full-thickness cutaneous wounds treated with (a) ASC or (b) ASC+EC on Integra, with Integra alone as a control. The ASC+EC treatment promoted a higher rate of wound closure compared to the control. The BLUE for the difference between the ASC+EC group and the Control group healing rates is -0.55 +/- 0.28 mm^2/day ($p = 0.017 < 0.025$, Bonferroni Adjusted), which is statistically significant. Bilateral wounds were made down thru the panniculus carnosus with a 3mm Acuderm biopsy punch tool on the dorsum of 18 NSG mice (9 male, 9 female), and then cut out using an Iris scissor. 6 mice received control (Integra scaffold with no cell treatment), 6 received Integra+ASC and 6 received Integra+ASC+EC. Wounds were covered with Tegaderm and bandaged with Vetrap. Images of the mouse wounds were taken at days 0, 7, 10, and 14 using a digital camera, and Image J was used to measure wound areas based on the images.

ASC treatment group and the Control healing rates is -0.45 +/- 0.22 mm^2/day. The p value was 0.041, which is not less than 0.025 and thus not statistically significant (Bonferroni Adjusted). The BLUE for the difference between the ASC+EC group and the Control group healing rates is -0.55 +/- 0.28 mm^2/day ($p = 0.017 < 0.025$, Bonferroni Adjusted), which is statistically significant.

This result suggests that the ASC+EC cell combination, which forms vascular networks, is contributing to graft vascularization and leading to more rapid re-epithelialization. An analysis of the histology confirmed this.

4.7 Presence of ASC and ASC+EC In Integra Graft Increases Revascularization In Cutaneous Full-Thickness Wounds

Noting the improved rate of wound healing for the ASC+EC treatment group, the histology was analyzed to look for differences between the treatments. The number of vessels was quantified (Figure 4.12) and revealed that ASC and ASC+EC treatment both stimulated increased vascularization compared to control (Integra scaffold alone). While there was no statistical difference in the number of vessels in ASC and ASC+EC treatment scaffolds, ASC+EC treatment had a higher number of vessels.

4.8 Supplementary Results

4.8.1 Seeding Three Cell Types on Integra

Apligraf and Orcel are two commercially available wound healing scaffolds that are seeded with keratinocytes before being applied to wounds [14, 20]. Noting their importance in the wound healing process, this is no surprise. As a pilot study, we investigated the possibility of seeding keratinocytes along with ASC+EC onto Integra to deliver both revascularization and re-epithelialization potential to wounds. After 2 days, ASC, EC, and keratinocytes are present on the scaffold (Figure 4.14 as cap-

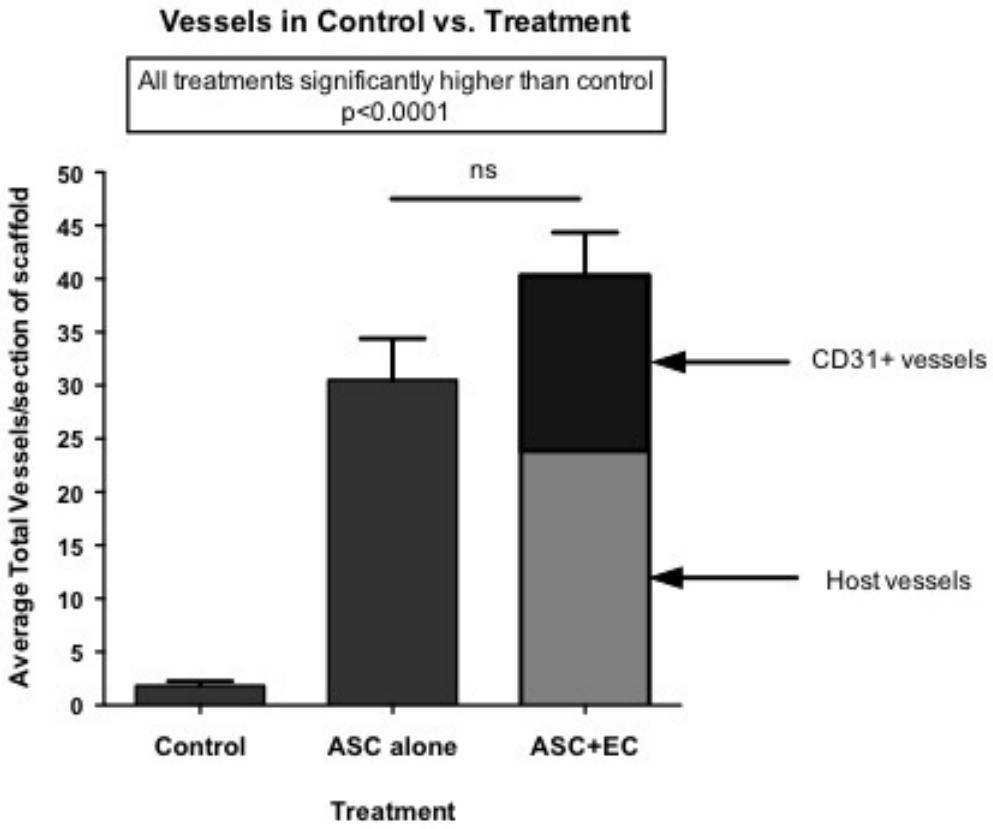

Fig. 4.12. ASC and ASC+EC treated scaffolds are more highly vascularized than the control scaffolds. Integra scaffolds seeded with ASC and ASC+EC were placed in murine full-thickness wounds. At Day 20, grafts were harvested, fixed, sectioned, stained (H&E, hCD31) and counted for mouse and human vessels. There were 10 sections of tissue analyzed for each graft in 10 different regions of the scaffold.

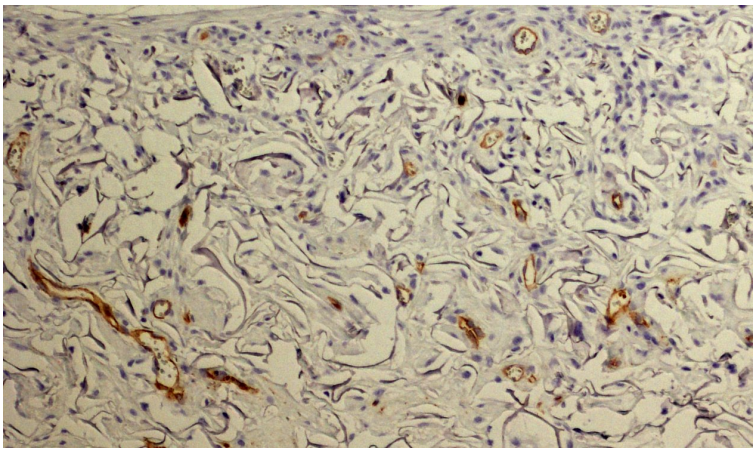

Fig. 4.13. hCD31 staining on ASC+EC treatment scaffolds reveals vessels formed by human EC (brown)

tured through fluorescent microscopy. Delivery of all three cell types via Integra is a consideration for future wound closure applications.

4.8.2 Feasibility of Spray Delivery of Cultured Cells and of SVF

ReCell® Spray-On Skin (Avita Medical, CA) utilizes spray technology to deliver keratinocytes to the site of debrided wounds. The process can be done at the bedside and fosters an even distribution of cells over the area of interest, which allows a very small skin biopsy to be used to cover a much larger area of skin. This has great potential as a replacement for skin grafts in wounds, especially when large areas of skin have been damaged. Dermal matrices such as Integra can be used to help repopulate lost tissue volume and ReCell® used to deliver the epidermal layer once the graft has become vascularized. With this in mind, we wanted to evaluate whether spray is a feasible method for delivery of ASC, EC and keratinocytes. In order to do this, we used transduced GFP-ASC, DsRed-EC, and unstained keratinocytes. Figure 4.15 shows images of sprayed vs. dripped cells. These images were formed by merging GFP (ASC) image, DsRed (EC) image and light microscope image (keratinocytes). Figure 4.16 shows a quantification of surviving cells determined by taking nine 20x images of each well and dividing cell counts by the area covered by each image. It does not appear that there is a relevant difference in cell survival between the two methods.

Based on our observation that ASC+EC promote an improvement in wound closure rate, and that they appear unaffected by being pushed through the Recell® nozzle, we wanted to assess the feasibility of delivering SVF via Recell®. SVF is attractive because it can be delivered at the bedside, and has all of the components necessary to form microvessels. Lectin staining revealed that spraying does not appear to affect SVF's vessel-forming capability (Figure 4.17).

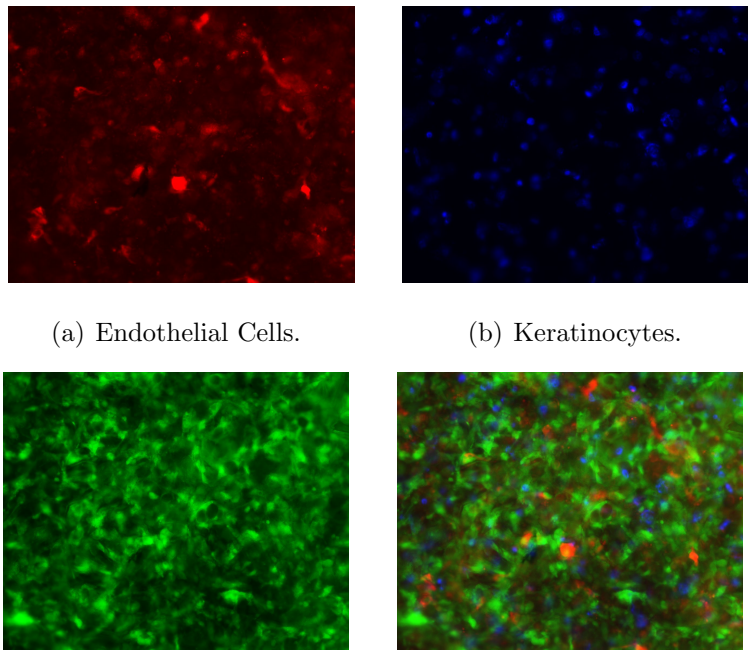

(a) Endothelial Cells. (b) Keratinocytes.

(c) ASC. (d) Three images merged.

Fig. 4.14. Three cell types on Integra scaffold (10x). (a) DsRed-EC, red, (b) DiD stained Keratinocytes, digitally colored blue, and (c) GFP-ASC, green were seeded onto Integra scaffold. (d) At day 2, representative images were taken (10x) and merged.

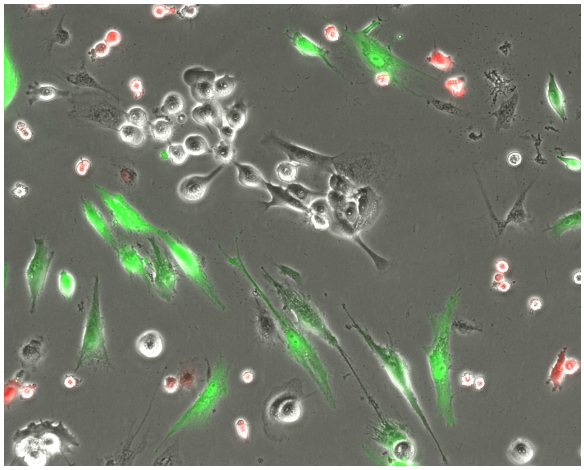

(a) Sprayed cells.

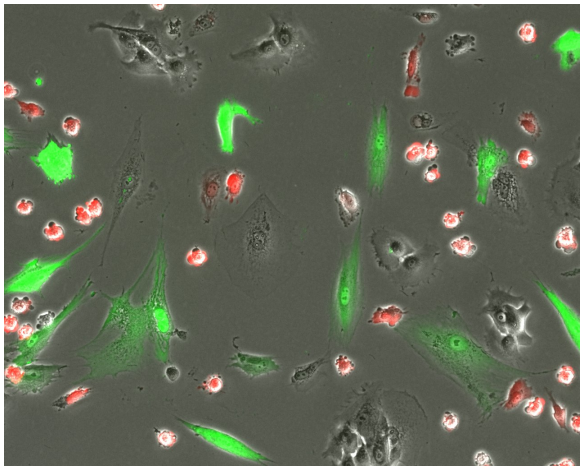

(b) Dripped cells.

Fig. 4.15. Cultured cells (a) sprayed with ReCell® vs. (b) dripped. Cell survival was not diminished by spraying. Equal numbers of keratinocytes (unlabeled), GFP-ASCs (green) and DsRed-ECs (red) were mixed and sprayed using ReCell® spray nozzle or dripped using a syringe and transferred to a 6 well plate. The next day, nine 20x images of the wells were taken and cell number quantified. Images formed by merging GFP (ASC) image, DsRed (EC) image and light microscope image (keratinocytes unstained).

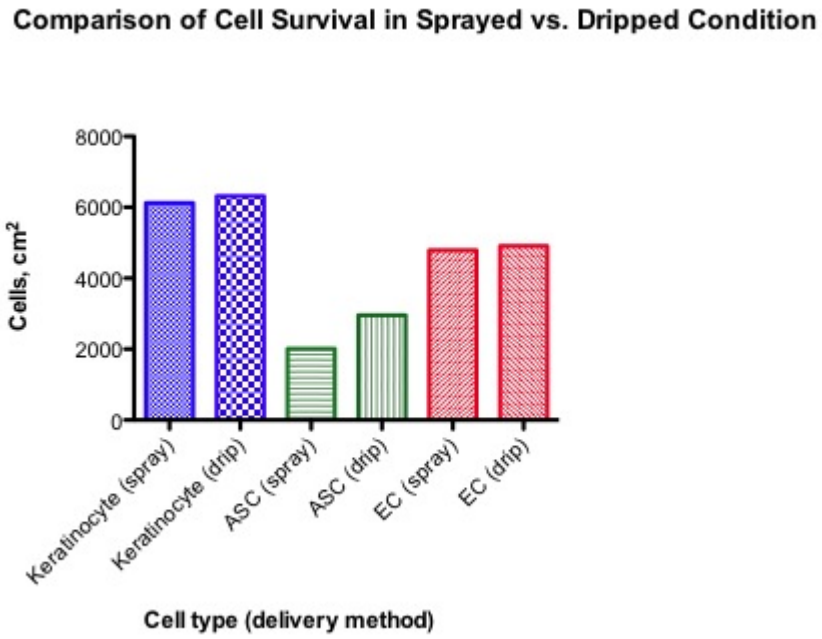

Fig. 4.16. Cultured cells sprayed and dripped together. Cell survival was not significantly diminished by spraying. Keratinocytes (unlabeled), GFP-ASCs and DsRed-ECs were mixed and sprayed using ReCell® spray nozzle or dripped using a syringe and transferred to a 6 well plate. The next day, nine 20x images of the wells were taken and cell survival quantified.

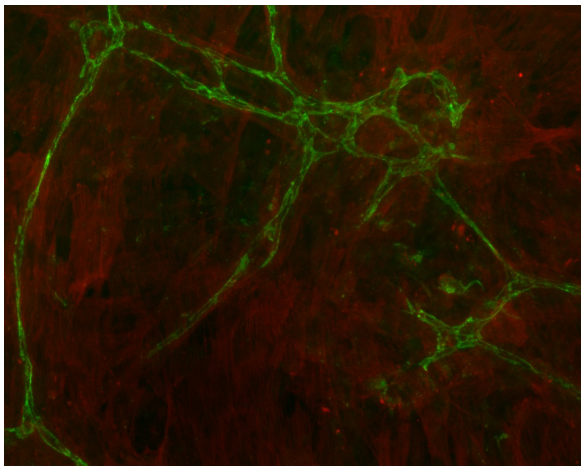

Fig. 4.17. Spraying SVF using ReCell® does not affect its ability to form microvessels. Sprayed SVF is stained after 6 days for lectin (10x image)

5. DISCUSSION

This study aimed to evaluate the potential of using ASC alone and ASC in combination with EC to promote graft revascularization. We hypothesized that ASC would promote revascularization of the dermal matrices by their paracrine activity. We also hypothesized that the ASC+EC combination would enhance and facilitate EC re-organization into vascular networks, thus improving graft revascularization. Histology revealed that both ASC and ASC+EC treatment groups had significantly more vessels in Integra scaffolds, compared to the control, though only ASC+EC case showed an improved rate of wound closure (compared to the control).

While ASC as a singular cell type has shown much potential in the arena of wound healing, the microvessel forming capabilities of ASC+EC when seeded on Integra is compelling. Rapid formation of robust, intact microvessel networks in a graft could enhance graft take and wound healing rate, especially in areas of low vascularity. However, one of the caveats of the use of cord-blood derived EC is that they are an allogeneic source, and thus will need to be HLA host/donor matched to reduce the chance for immune rejection. These EC are highly proliferative and easy to expand, so banking them for cell delivery applications is very feasible. Additionally, ASC have been shown to have immunosuppressive and anti-inflammatory properties [46,47]. Thus, we speculate that delivery of EC along with ASC may alter the immune response elicited by ECs' allogeneic origins.

With 1 million burn injuries reported annually [12–14] and 45,000 hospitalizations due to fires and burns, the importance of having an effective treatment for severe second-degree and third-degree burn wounds is critical. Skin grafts are a current treatment for these types of wounds [16, 18], but there are several drawbacks associated with their use including a lack of availability of suitable donor sites for autografts in some instances, rejection and possible transfer of infection associated

with allografts and xenografts, and poor graft retention due to infection, hematoma and low vascularity at the recipient site. As such, research has been done into the use of artificial skin substitutes as a burn treatment. They are readily available, encourage in-growth of surrounding cells, and can be loaded with specialized cells or growth factors that stimulate faster healing, prevent fluid loss, and reduce scarring [17,20,21]. Skin substitutes can be subdivided into three major categories, including acellular, cellular and cellular autologous [20]. Integra and Alloderm are acellular skin substitute, indicated for use in a wide array of wound healing applications including burn wounds. We successfully cultured ASC and ASC+EC on these scaffolds.

In an effort to preserve the integrity of the Integra matrix, and to mimic its clinical use as closely as possible, we did not remove the silicone backing before implanting them into the mouse full-thickness wounds. When Integra is used in clinic, the silicone layer is only removed after the scaffold has successfully integrated with the host, and is ready for application of a thin epidermal autograft [48]. The silicone layer serves as a barrier to pathogens and helps retain moisture. In our model, the Integra scaffolds were placed in the wound, with silicone side down, and dermal side facing up. While perhaps not the ideal setup for a mouse wound healing model, this was done to mimic clinical applications of Integra as much as possible. This means that host vascularization and cellular in-growth was inhibited from below and limited to lateral and top-side penetration.

Noting the vessel forming dynamics of EC in the presence of ASC, when cultured on Integra and Alloderm, we speculate on the possibility of generating scaffolds with pre-formed microvessel networks and applying these to wounds. This is an area that needs further exploration. Perhaps there is an advantage to delivering intact vascular networks to the site of wounds. On the other hand, effective microvessel formation and integration with host may be a factor of ASC and EC interactions with their environment as they are forming vessels. In this same vein, we considered the possibility of using fluid flow to control the orientation of the networks. Vessel orientation may be another factor that may enhance graft revascularization via host.

Perhaps vessels all oriented parallel or all at right angles to the site of injury, rather than randomly, will integrate more easily with host vasculature. Much work was done to generate flow-oriented microvessel networks on tissue culture plastic (See summary in the Appendix). While largely unrepeatable, the results are presented here as they may offer a framework for continuing this work and expanding it to a 3D model.

Initial experiments done with ASC and ASC+EC conditioned media also revealed that their secreted factors increased survival and migration of keratinocytes. Keratinocytes form the outer layers of epidermis and thus play an important role in the wound healing process. It's noteworthy that both ASC and ASC+EC conditioned media had similar migratory and survival effects on keratinocytes. It suggests that by 72 hours (length of incubation to generate conditioned media) there are no significant differences in accumulation of critical factors. For the VEGF secretion profile on Integra (Figure 4.8(a)), major changes in accumulation only occurred after 72 hours.

The murine model used to study wound closure had some limitations. There are several structural and physiological differences in the skin and in the wound healing process of mice vs. humans. One of these is the tendency of mouse wounds to heal primarily via contraction and less via re-epithelialization. Galiano et. al. attempted to address this limitation through the use of silicone disks sutured around the wound site as a splint [49], but we found this method difficult to apply to our model. Instead, we used tegaderm as a splinting material as has been done in a previous study [50]. In a brief experiment we performed (results not shown), we confirmed that tegaderm splinted wounds had a significantly decreased rate of wound healing compared to unsplinted wounds, most likely due to a reduction in wound contraction. During the study, mice had to be monitored daily to ensure that they did not remove their bandages and the underlying tegaderm. If the bandages were removed, mice were placed under anesthesia and the bandages reapplied.

In spite of some of the limitations of our model, it is very promising that even in this healthy murine model with normal skin, the ASC+EC treatment group showed a statistically significant increase in wound closure rate and greater amount of vas-

cularity in the Integra scaffold compared to the cell-free control. We would expect to see an even greater enhancement in a delayed wound-healing model. Study of such a model would serve to validate our findings and provide opportunity for further study of the mechanism of improved wound healing in ASC + EC treatment delivered via Integra. An irradiated porcine model as described by Hadad, et. al. [34] would be an excellent next step due to (1) the physiological and wound healing similarities between porcine skin and human skin and (2) the impaired wound healing caused in large part by a reduction in vascular perfusion due radiation exposure.

ASC+EC on Integra could be a possible treatment for full-thickness burn wounds where application of a skin graft is unsuitable or in regions of low vascularity. Integra is already indicated for use in third degree burns and delivery of autologous ASC and readily available allogeneic EC to the site of the wound may prove efficacious due to their vessel forming capabilities. It is well documented that poor vascularization is a major contributor to graft failure, and that restoration of vascular perfusion is critical in the wound healing process.

5.1 Future Direction

Based on the findings presented in the supplementary results, three ideas can be further explored. First, spray technology as a delivery mechanism for keratinocytes may be used in place of a skin graft in wounds treated with a dermal template, such as Integra. Normally, after Integra becomes adequately vascularized, the silicone backing is removed and a thin epidermal graft is applied for re-epithelialization. In the case of burn wounds, if suitable donor skin availability is low due to extensive burning, a small biopsy of skin can be taken and spray delivered to improve coverage.

Second, an alternative worth exploring is the delivery of ASC and ASC+EC in combination with keratinocytes on Integra scaffold in a one-step application. We have shown that seeding ASC+ EC+ keratinocytes on Integra is feasible. This may

not only enhance vascularization (ASC or ASC+EC) but also re-epithelialization (keratinocytes) and may remove the need for a second-step skin graft application.

Finally, the use of SVF in place of expanded and cultured ASC and ASC+EC should be explored since it cuts down on time for expansion and isolation of pure ASC and EC populations and can be delivered within hours of obtaining adipose tissue from a patient.

LIST OF REFERENCES

LIST OF REFERENCES

[1] F. C. Brunicardi, D. K. Andersen, T. R. Billiar, D. L. Dunn, J. G. Hunter, J. B. Matthews, and R. E. Pollock, *Schwartz's Principles of Surgery, 9e.* Columbus, OH: McGraw-Hill Education, ninth ed., 2010.

[2] P. Sipos, H. Gyry, K. Hagymsi, P. Ondrejka, and A. Blzovics, "Special wound healing methods used in ancient egypt and the mythological background," *World Journal of Surgery*, vol. 28, no. 2, pp. 211–216, 2004.

[3] H. W. Hopf, L. M. Humphrey, N. Puzziferri, J. M. West, C. E. Attinger, and T. K. Hunt, "Adjuncts to preparing wounds for closure: hyperbaric oxygen, growth factors, skin substitutes, negative pressure wound therapy (vacuum-assisted closure)," *Foot and Ankle Clinics*, vol. 6, no. 4, pp. 661–682, 2001.

[4] S. C. Wu, W. Marston, and D. G. Armstrong, "Wound care: The role of advanced wound healing technologies," *Journal of Vascular Surgery*, vol. 52, no. 3, pp. 59S–66S, 2010.

[5] B. Alberts, A. Johnson, and J. Lewis, *Epidermis and Its Renewal by Stem Cells (in): Molecular Biology of the Cell.* Garland Science, fourth ed., 2002.

[6] C. M. Chuong, B. J. Nickoloff, P. M. Elias, L. A. Goldsmith, E. Macher, P. A. Maderson, J. P. Sundberg, H. Tagami, P. M. Plonka, K. Thestrup-Pedersen, B. A. Bernard, J. M. Schrder, P. Dotto, C. H. Chang, M. L. Williams, K. R. Feingold, L. E. King, A. M. Kligman, J. L. Rees, and E. Christophers, "Contoversies in experimental dermatology: What is the true function of skin?," *Experimental Dermatology*, vol. 11, no. 2, pp. 159–187, 2002.

[7] L. A. Brodell and K. S. Rosenthal, "Skin structure and function: The body's primary defense against infection," *Infectious Diseases in Clinical Practice*, vol. 16, no. 2, pp. 113–117, 2008.

[8] S. Guo and L. A. DiPietro, "Factors affecting wound healing," *Journal of Dental Research*, vol. 89, no. 3, pp. 219–229, 2010.

[9] A. Gosain and L. A. DiPietro, "Aging and wound healing," *World Journal of Surgery*, vol. 28, no. 3, pp. 321–326, 2004.

[10] M. Mercandetti, "Wound healing and repair," *WebMD*, 2013.

[11] L. A. DiPietro, M. Burdick, Q. E. Low, S. L. Kunkel, and R. M. Strieter, "Mip-1alpha as a critical macrophage chemoattractant in murine wound repair," *The Journal of Clinical Investigation*, vol. 101, no. 8, pp. 1693–1698, 1998.

[12] C. G. Mayhall, "The epidemiology of burn wound infections: Then and now," *Clinical Infectious Diseases*, vol. 37, no. 4, pp. 543–550, 2003.

[13] E. A. Deitch, "The management of burns," *The New England Journal of Medicine*, vol. 37, no. 4, pp. 543–550, 1990.

[14] D. M. Supp and S. T. Boyce, "Engineered skin substitutes: practices and potentials," *Clinics in Dermatology*, vol. 23, no. 4, pp. 403–412, 2005.

[15] A. S. Halim, T. L. Khoo, and S. J. M. Yussof, "Biologic and synthetic skin substitutes: An overview," *Indian Journal of Plastic Surgery*, vol. 43, pp. S23–S28, 2010.

[16] A. P. Sanford and D. N. Herndon, *Current Therapy of Burns (in): Surgical Treatment: Evidence-Based and Problem-Oriented*. Munich: Zuckschwerdt, 2001.

[17] D. G. Simpson, "Dermal templates and the wound-healing paradigm: the promise of tissue regeneration," *Expert Review of Medical Devices*, vol. 3.4, 2006.

[18] compiled by Peter Igneri and J. Gratton, *FAHC Burn Care Manual*. Fletcher Allen Health Care and The University of Vermont College of Medicine, 2008.

[19] D. Church, S. Elsayed, O. Reid, B. Winston, and R. Lindsay, "Burn wound infections," *Clinical Microbiology Reviews*, vol. 19, no. 2, pp. 403–434, 2006.

[20] L. Alrubaiy and K. K. Al-Rubaiy, "Skin substitutes: A brief review of types and clinical applications," *Oman Medical Journal*, vol. 24, no. 1, 2009.

[21] J. F. Thornton, "Skin grafts and skin substitutes," *Selected Readings in Plastic Surgery*, vol. 10, no. 1, 2004.

[22] J. Noordenbos, C. Dore, and J. Hansbrough, "Safety and efficacy of transcyte for the treatment of partial-thickness burns," *Journal of Burn Care Rehabilitation*, vol. 20, pp. 275–281, 1999.

[23] F. Bioscience, "What is orcel: Product description." `http://www.forticellbioscience.com/orcel.html`, 2008.

[24] H. Carsin, P. Ainauda, H. L. Bevera, J.-M. Rivesb, A. Lakhelb, J. Stephanazzia, F. Lambertb, and J. Perrot, "Cultured epithelial autografts in extensive burn coverage of severely traumatized patients: a five year single-center experience with 30 patients," *Burns*, vol. 26, no. 4, pp. 379–387, 2000.

[25] EpiCel, "Procurement procedure." `http://www.epicel.com/hcp/epicel-treatment/procurement.aspx`, 2013.

[26] P. L. K. Jr, "Skin grafts and skin substitutes," *Selected Readings in Plastic Surgery*, vol. 9, no. 1, 1999.

[27] D. O. Traktuev, D. N. Prater, S. Merfeld-Clauss, A. R. Sanjeevaiah, M. R. Saadatzadeh, M. Murphy, B. H. Johnstone, D. A. Ingram, and K. L. March, "Robust functional vascular network formation in vivo by cooperation of adipose progenitor and endothelial cells," *Circulation Research*, vol. 104, pp. 1410–1420, 2009.

[28] D. O. Traktuev, S. Merfeld-Clauss, J. Li, M. Kolonin, W. Arap, R. Pasqualini, B. H. Johnstone, and K. L. March, "A population of multipotent cd34-positive adipose stromal cells share pericyte and mesenchymal surface markers, reside in a periendothelial location, and stabilize endothelial networks," *Circulation Research*, vol. 102, pp. 77–85, 2008.

[29] P. Zhang, N. Moudgill, E. Hager, N. Tarola, C. DiMatteo, S. McIlhenny, T. Tulenko, and P. J. DiMuzio, "Endothelial differentiation of adipose-derived stem cells from elderly patients with cardiovascular disease," *Stem Cells and Development*, vol. 20, no. 6, pp. 977–988, 2011.

[30] L. J. Harris, P. Zhang, H. Abdollahi, N. A. Tarola, C. DiMatteo, S. E. McIlhenny, T. N. Tulenko, and P. J. DiMuzio, "Availability of adipose-derived stem cells in patients undergoing vascular surgical procedures," *Journal of Surgical Research*, vol. 163, no. 2, pp. 105–112, 2010.

[31] S. J. Hong, D. O. Traktuev, and K. L. March, "Therapeutic potential of adipose-derived stem cells in vascular growth and tissue repair," *Current Opinion in Organ Transplant*, vol. 15, no. 1, pp. 86–91, 2010.

[32] S. Merfeld-Clauss, N. Gollahalli, K. L. March, and D. O. Traktuev, "Adipose tissue progenitor cells directly interact with endothelial cells to induce vascular network formation," *Tissue Engineering Part A*, vol. 16, no. 9, pp. 2953–2966, 2010.

[33] M. W. Blanton, I. Hadad, B. H. Johnstone, J. A. Mund, P. I. Rogers, B. L. Eppley, and K. L. March, "Adipose stromal cells and platelet-rich plasma therapies synergistically increase revascularization during wound healing," *Plastic Reconstructive Surgery Journal*, vol. 123, no. 2S, 2009.

[34] I. Hadad, B. H. Johnstone, J. G. Brabham, M. W. Blanton, P. I. Rogers, C. Fellers, J. L. Solomon, S. Merfeld-Clauss, C. M. DesRosiers, J. R. Dynlacht, J. J. Coleman, and K. L. March, "Development of a porcine delayed wound-healing model and its use in testing a novel cell-based therapy," *International Journal of Radiation Oncology Biology Physics*, vol. 78, no. 3, pp. 888–896, 2010.

[35] P. J. Amos, S. K. Kapur, P. C. Stapor, H. Shang, S. Bekiranov, M. Khurgel, G. T. Rodeheaver, S. M. Peirce, and A. J. Katz, "Human adipose-derived stromal cells accelerate diabetic wound healing:impact of cell formulation and delivery," *Tissue Engineering: Part A*, vol. 16, no. 5, pp. 1595–1606, 2010.

[36] C. Nie, D. Yang, J. X, Z. Si, X. Jin, and J. Zhang, "Locally administered adipose-derived stem cells accelerate wound healing through differentiation and vasculogenesis," *Cell Transplantation*, vol. 20, pp. 205–216, 2011.

[37] C. Nie, G. Zhang, D. Yang, T. Liu, D. Liu, J. Xu, and J. Zhang, "Targeted delivery of adipose-derived stem cells via acellular dermal matrix enhances wound repair in diabetic rats," *Journal of Tissue Engineering and Regenerative Medicine*, 2012.

[38] M. Cherubino, J. P. Rubin, N. Miljkovic, A. Kelmendi-Doko, and K. G. Marra, "Adipose-derived stem cells for wound healing applications," *Annals of Plastic Surgery*, vol. 66, no. 2, 2011.

[39] W.-S. Kim, B.-S. Park, J.-H. Sung, J.-M. Yang, S.-B. Park, S.-J. Kwak, and J.-S. Park, "Wound healing effect of adipose-derived stem cells: a critical role of secretory factors on human dermal fibroblasts," *Journal of Dermatological Science*, vol. 48, no. 1, pp. 15–24, 2007.

[40] S. H. Lee, S. Y. Jin, J. S. Song, K. K. Seo, and K. H. Cho, "Paracrine effects of adipose-derived stem cells on keratinocytes and dermal fibroblasts," *Annals of Dermatology*, vol. 24, no. 2, pp. 136–143, 2012.

[41] F. M. Wood, N. Giles, A. Stevenson, S. Rea, and M. Fear, "Characterization of the cell suspension harvested from the dermal epidermal junction using a recell®kit," *Burns*, vol. 38, pp. 44–51, 2012.

[42] R. Sheridan, J. Morgan, J. Cusick, L. Petras, M. Lydon, and R. Tompkins, "Initial experience with a composite autologous skin substitute," *Burns*, vol. 75, pp. 421–424, 2001.

[43] P. Clugston, C. Snelling, I. Macdonald, and H. Maledy, "Cultured epithelial autografts: three years of clinical experience with eighteen patients," *Journal of Burn Care Rehabilitation*, vol. 12, pp. 533–539, 1991.

[44] M. Desai, J. Mlakar, R. McCauley, K. Abdullah, and R. Rutan, "Lack of long-term durability of cultured keratinocyte burn-wound coverage: a case report," *Journal of Burn Care Rehabilitation*, vol. 12, pp. 540–545, 1991.

[45] H. Motulsky and A. Christopoulos, *Fitting Models to Biological Data Using Linear and Nonlinear Regression: A Practical Guide to Curve Fitting*. Oxford University Press, 1 ed., 2004.

[46] B. Puissant, C. Barreau, P. Bourin, C. Clavel, J. Corre, C. Bousquet, C. Taureau, B. Cousin, M. Abbal, P. Laharrague, L. Penicaud, L. Casteilla, and A. Blancher, "Immunomodulatory effect of human adipose tissue-derived adult stem cells: comparison with bone marrow mesenchymal stem cells," *British Journal of Hematology*, vol. 129, pp. 118–129, 2005.

[47] H.-J. Lee, M. Jung, J.-H. Kim, N. young Yoon, and E. H. Choi, "The effect of adipose-derived stem cell-cultured media on oxazolone treated atopic dermatitis-like murine model," *Annals of Dermatology*, vol. 24, pp. 181–188, 2012.

[48] I. L. Corporation, "Product information." `http://www.integralife.com/index.aspx?redir=Burn-Care`, 2013.

[49] R. Galiano, t. J Michaels, M. Dobryansky, J. Levine, and G. Gurtner, "Quantitative and reproducible murine model of excisional wound healing," *Wound Repair and Regeneration*, vol. 12, no. 4, pp. 485–492, 2004.

[50] T.-Y. Chung, P. V. Peplow, and G. D. Baxter, "Laser photobiostimulation of wound healing: Defining a dose response for splinted wounds in diabetic mice," *Lasers in Surgery and Medicine*, vol. 42, pp. 816–824, 2010.

APPENDIX

APPENDIX: USE OF FLOW-GENERATED SHEAR STRESS TO CONTROL ORIENTATION OF MICROVESSEL NETWORKS

A.1 Author's Note

Looking at using shear stress generated by laminar fluid flow to align ASC-EC microvessels was the project I first started out with. However, I quickly ran into difficulties with contamination and then reproducibility. I attempted to find a flow chamber that would allow me to successfully perform long-term flow analysis (3-6 days) while maintaining sterility. Then, once I got my hands on such a machine (Cellmax Flow pump with ibidi cell culture chambers), I was able to observe ASC alignment once, but could not reproduce it with the same or other donor ASC. It seemed this project was destined to be a challenge from the start. In the end, after many months of investigating new flow pumps and new strategies we switched to a much simpler model, using an orbital shaker, and were able to reproduce the outcome of flow aligned ASCs. However, there still remains a high degree of variability in the outcomes. In conclusion, we were able to demonstrate the alignment of microvessels formed by seeding ECs on flow aligned ASCs. Overall, this project reached a temporary hold in favor of the wound healing project, but are interestingly linked as we consider the possibility of generating pre-aligned vessel networks and applying these to wounds.

A.2 Hypothesis

We hypothesized that due to its physiological influence, fluid shear stress may have an effect on microvessel formation in vitro, impacting amongst other factors,

microvessel network orientation. With this in mind, the first aim was to determine if fluid flow could be used to control ASC orientation.

This work could have application in tissue engineering. The ability to control the structure and orientation of vessels could be useful when attempting to grow organs out of the body for implantation purposes.

A.3 Methods and Results

The basic experimental design was to seed ASC, EC and ASC+EC co-cultures confluently onto the slide or flow area, allow them to attach overnight and then apply shear stress.

Several different systems were investigated for studying fluid flow on ASC and ASC+EC. All worked on the same basic premise of using a pump to move fluid from a reservoir thru the cell chamber where the cells were grown, and could experience the shearing force. The microfluid device used a vacuum to attach the flow chamber to a petri dish (Figure A.1). Cells were seeded into a small rectangular area where fluid was made to pass using a roller pump. The device was housed in a 5% Carbon dioxide incubator to maintain ambient temperatures and pH. The second flow chamber used differences in height and a roller pump to move fluid into the cell chamber (Figure A.2). The cells were seeded onto glass slides and the slides inserted into the cell chamber, which contained openings to allow media to flow over the cells, generating a shear stress. The height of the reservoir could be adjusted to control the shear stress.

Unfortunately, none of these systems were designed for long-term culture and I had great difficulties running the experiment for more than a day or two before contamination set in. No alignment was observed in these experiments.

The third system we worked with was designed for long-term culture under flow. It was a demo device we got to use for a month, obtained from Ibidi. They had special culture slides that allowed cells to be grown as a monolayer, and media passed over them via a pump system, to generate the shear stress. I had little success with the

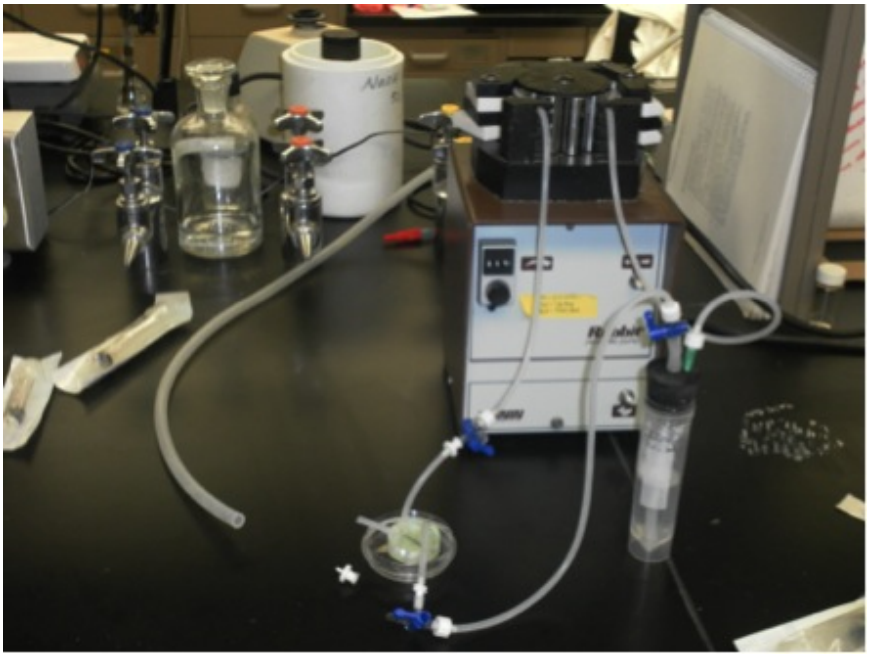

Fig. A.1. Microfluid flow device set-up.

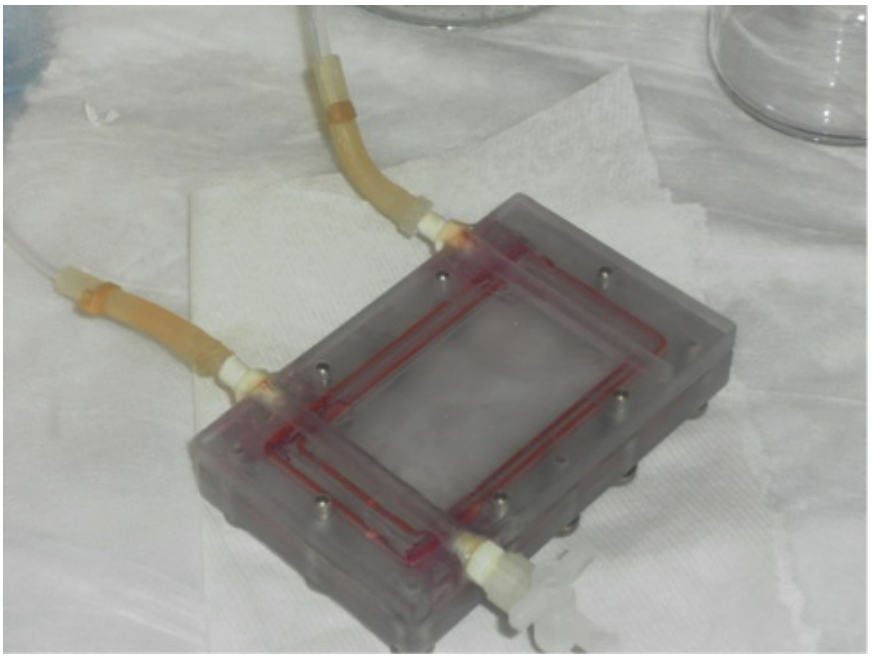

Fig. A.2. Cell chamber used in laminar flow system developed by Dr. Ji's reasearch team in Engineering

ibidi pump system before the demo period was up, but I learned how to use the slides more effectively. In the fourth system, I used a flow pump developed by CellMax to generate the shear stress, and used the ibidi slides to culture the cells. It was in this system that I was first able to capture ASC alignment over a 6-day period (Figure A.3). GFP-labeled ASC were allowed to attach overnight and then flow was applied the next day. Images were taken with a Nikon Ti. Change in angle of orientation of cells was measured using Image J (Figure A.4).

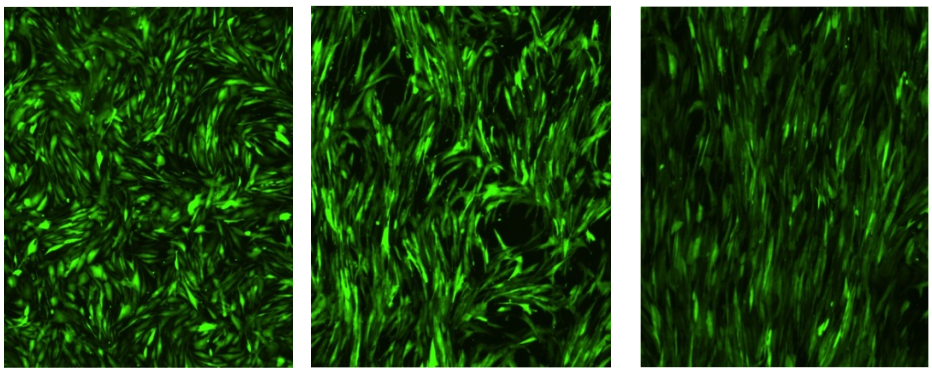

(a) Day 0 (b) Day 1 (c) Day 2

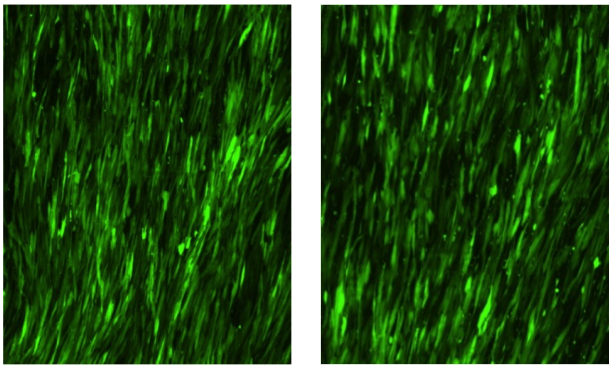

(d) Day 3 (e) Day 6

Fig. A.3. GFP-labeled ASC seeded into ibidi chamber and aligned using shear stress over a 6 day period.

Unfortunately, I was never able to reproduce this result using the Cellmax flow pump system, which raised a number of questions about conditions necessary for ASC alignment. Additional ASCs were put under shear stress, but no alignment was

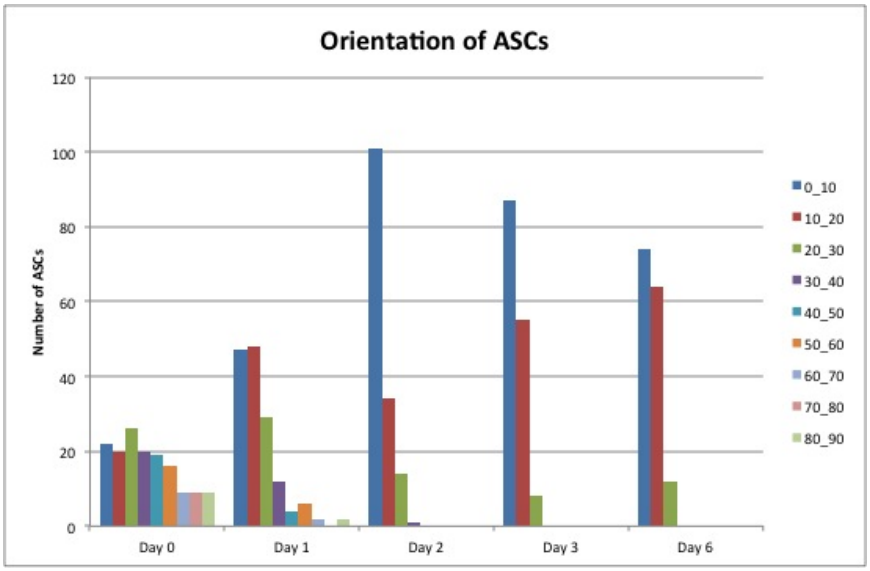

Fig. A.4. Change in orientation angle of ASC over 6 day period of exposure to flow

observed. This raised further questions about ASC response to shear stress. Perhaps the initial outcome was an artifact due to over-culturing or some other phenomenon.

The next thing we attempted was very simple and was where we likely should have started. We used an orbital shaker to generate shear stress on the cells, by seeding them onto petri dishes and attaching them to the orbital shaker. Now, we had a simple system to use and set-up with low incidence of contamination. The variable shear stress along radius r, was initially why it was not chosen as the flow system of choice. But, for achieving the aim of aligning microvessel networks, it proved useful.

However, the variability in ASC response continued. Many experiments were run to test different donors, different ASC attachment times, different shear stresses and different seeding densities, but nothing conclusive could be derived. Figure 20 shows the most successful and promising outcome. It was set up as follows: 60k/cm^2 ASC seeded, allowed 3 hours to attach and then put under rotational flow for 4 days. At the end of this, 10k/cm^2 EPC were added and incubated for 6 days in EBM-2, 5% FBS (static). DsRed ECs were used. See the results in Figure A.5. The outcome is that flow aligned ASCs can be used to control the orientation of resulting microvessel networks.

Now that we know this is possible, future plans would be to attempt to apply this to a 3D model using a porous scaffold. Further work must also be done to elucidate the secrets of the ASC flow-response, which seems quite variable and unpredictable at present.

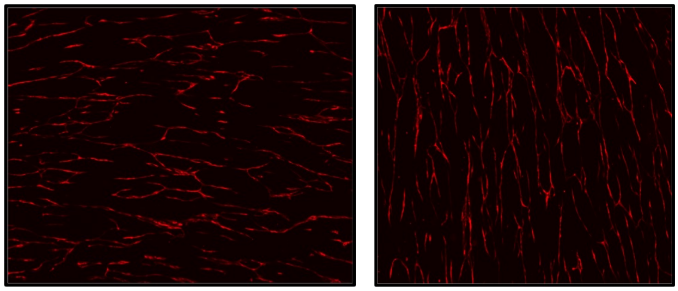

(a) 12noon position of circle (b) 3pm position of circle

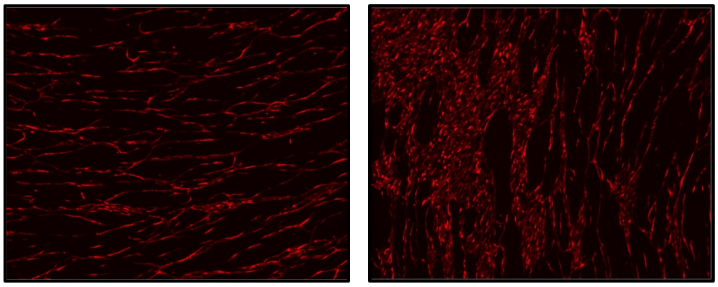

(c) 6pm position of circle (d) 9pm position of circle

Fig. A.5. Flow aligned ASC produce flow aligned microvessels.